# Protocols for Reproducible, Increased-Scale Synthesis of Engineered Particles – Bridging the "Upscaling Gap"

Steve Spoljaric, Yi Ju, and Frank Caruso*

ARC Centre of Excellence in Convergent Bio-Nano Science and Technology, and the Department of Chemical Engineering, The University of Melbourne, Parkville, Victoria 3010, Australia

**ABSTRACT:** Large-scale, reproducible synthesis of particles is key to achieving broader material accessibility and applicability. However, direct scaling of experimental parameters, such as reagent volume, does not always translate to the corresponding product yields and/or material property profiles. This is particularly relevant for particle systems, of which the properties and subsequently quality and application are determined from the synthesis methodology. Herein, large-scale synthesis protocols for the template-directed assembly of three particle systems used in our laboratory are detailed, and challenges and considerations with the assembly methods are discussed. These particle systems have potential in targeted drug delivery, imaging and catalysis, as functional coatings, and for heavy metal ion removal applications. The discrete assembly of metal–phenolic network (MPN) films on polystyrene (PS) templates is first detailed, followed by the self-assembly of MPN films onto oil/water emulsions, and finally the fabrication of silica supraparticles (Si-SPs) via gel-mediated electrospraying. For both MPN techniques, significant increases in yield (>450-fold for discrete assembly onto PS templates and 2-fold for self-assembly onto oil/water emulsions) were obtained without significant discrepancies in capsule properties. Similarly, up to a 4-fold increase in Si-SP yield (per hour) was achieved via gel-mediated electrospraying without significant deviations in particle properties. A series of detailed, stepwise protocols are presented for each particle system with accompanying video footage. Challenges and considerations are discussed for each particle synthesis protocol, with strategies for mitigating issues and ensuring particle reproducibility and quality. These protocols are designed to be straightforward to implement by researchers with little-to-no prior experience in particle engineering, so as to promote the broad application of these particle systems.

## 1. INTRODUCTION

Engineered particles show potential in a range of different applications, including drug delivery,[1–4] anti-biofouling,[5–8] biomedical imaging,[9–12] enzyme immobilization,[13–15] catalysis,[16,17] functional coatings,[18-20] and heavy metal ion removal.[21,22] This breadth and appeal have spurned interest[23–28] and have created a need for the reproducible production of these materials at increased yields. The potential for upscaling is determined by various factors, including the methods used to synthesize the particles (as particle properties are often dictated by the synthesis methodology), the ease with which the methods can be adapted, and the availability of equipment and reagents. Most importantly, ensuring reproducibility in every batch is essential for conducting accurate, efficient, and timely studies.

The scientific literature provides detailed synthesis protocols (complemented in several cases by video footage) of a range of synthesis techniques, including layer-by-layer assembly, mesoporous silica replication,[29] electrospraying assembly,[30] and template-mediated discrete assembly (e.g., for the preparation of metal–phenolic networks (MPNs)).[29] However, these methods are only optimal for the production of small-scale yields (i.e., several milligrams or micrograms) rather than large laboratory-scale yields (i.e., tens/hundreds of milligrams to 1–2 g). For example, mixing/dispersion efficiency and supernatant removal following centrifugation (without disturbing the particle pellet) can be challenging when volumes and scales are increased above the milligram range. This not only affects yield recovery, but also can be detrimental to reproducibility. Furthermore, onboarding and protocol familiarization on the part of new researchers entering a new research field can be timely and costly, particularly when the researchers who originally developed these methods are no longer present.

To bridge this "upscaling gap" from yields on the order of several micro- or milligrams to grams, method validation and benchmarking using (where possible) commonly available/accessible laboratory equipment and materials, and providing unambiguous and detailed protocols provide a pathway to ensure high reproducibility, while limiting time investment and material expenses. These protocols can also serve as a stepping stone to pilot-scale synthesis protocols and yields.

Herein, protocols were developed to reproducibly synthesize a range of engineered particles at increased yields, including:

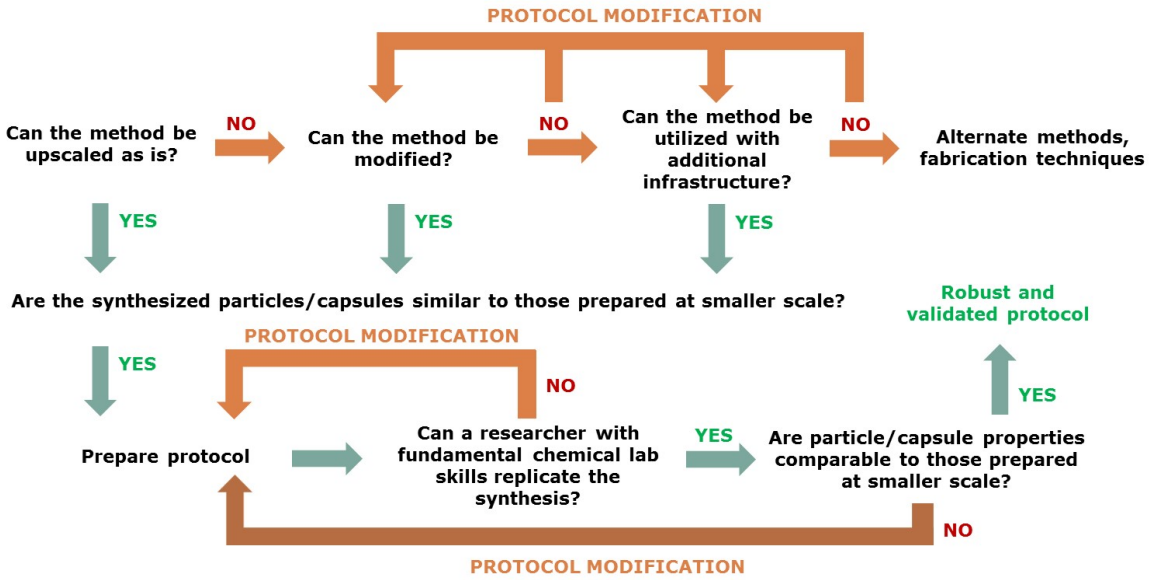


**Scheme 1. Flow chart summarizing the pathway used to prepare protocols for reproducible, large-scale synthesis of particles/capsules.**

- MPNs via discrete assembly on spherical polystyrene (PS) templates based on the protocol of Ejima et al.[31] and Björnmalm et al.[29]
- MPNs via interfacial self-assembly on oil-in-water (oil/water) emulsions based on the protocol of Besford et al.[7]
- Silica supraparticles (Si-SPs) via gel-mediated electrospraying assembly based on the protocol of Ma et al.[30]

The referenced protocols were selected because of their robustness and reproducibility; however, they have been optimized for the fabrication of particles and capsules at milligram or microgram scales. Therefore, the present manuscript will focus on scaling these published methodologies to fabricate particles/capsules at increased yields, while also comparing the properties and characteristics of the particles/capsules with the published data to confirm successful protocol development and reproducibility. Scheme 1 summarizes the strategic pathway used to develop and validate the protocols for reproducible, large-scale particle/capsule synthesis.

The criteria for the developed protocols were as follows:

- sufficiently robust to ensure high reproducibility and high yields for each synthesis;
- clear, easy to follow, and detailed, readily understood and adapted by a researcher with basic chemistry laboratory skills; and
- can be readily performed and adapted in most, if not all, academic chemistry/materials science laboratories.

For each protocol, an overview is presented, followed by a step-by-step guide using a particle model system. Common challenges, obstacles, and other considerations are discussed. To confirm robustness of the methods as well as accessibility to the broader scientific community, the protocols are followed and undertaken by a researcher with basic chemistry laboratory skills and no prior experience in particle engineering. Video footage of the synthesis protocols is provided to complement the protocols. The goal is to provide detailed and clear instructions, as well as highlight hindrances and pitfalls, to assist with efficient particle engineering in academic chemistry/materials science laboratories.

## 2. TEMPLATE-MEDIATED DISCRETE ASSEMBLY OF MPNs

### 2.1. Overview

MPNs are supramolecular network structures formed via pH-dependent coordination chemistry involving transition metal ions and polyphenol ligands. The mechanism of formation involves simultaneous adsorption of polyphenols and their subsequent cross-linking by metal ions, resulting in three-dimensional, stable network structures (Figure 1). Specifically, the hydroxyl groups of the catechol and galloyl moieties within the polyphenol ligands coordinate to the metal ions. MPN films have been successfully deposited onto a range of planar substrates, and inorganic, organic, and biological templates of different shapes, sizes, dimensions, and surface chemistry.[32–34] MPN microcapsules are obtained via coating of spherical micro-templates and subsequent template dissolution,[35] which will be the focus of this section. The synthesis involves a rapid, one-step mixing of metal and ligand solutions, yielding films with a thickness of ~10 nm within minutes on the templates.[31] Film thickness (and properties influenced by film thickness such as permeability and mechanical strength) can be altered by exposing the template substrate repeatedly to the ligand and metal solutions,[32,36] thereby resulting in a multi-step synthesis process. Both the single- and multi-step synthesis routes are inexpensive, require minimal energy input, and are environmentally sustainable when using plant-derived polyphenols such as tannic acid (TA) and gallic acid.

MPNs consisting of $Fe^{III}$ and TA have been the most thoroughly studied, although a range of ligands and metals have been used to prepare MPNs,[12,37,38] with each metal–ligand combination (as well as synthesis method) showcasing its own

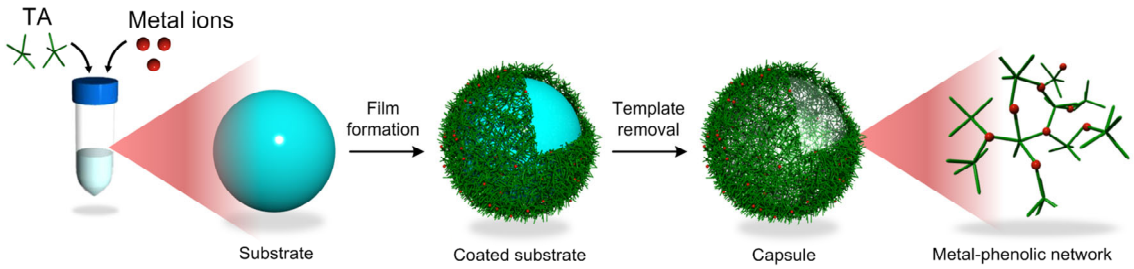


**Figure 1.** Overview of the discrete assembly of MPNs onto a spherical template. Reproduced with permission from reference.[12] Copyright 2014 Wiley-VCH Verlag GmbH & co.

specific properties and characteristics. Furthermore, the ability to functionalize molecules with catechol or galloyl groups expands the potential number of ligand candidates, as well as properties and applications of the resulting MPN systems. As an example, low-fouling MPN particles with high targeting specificity to cancer cells were prepared via complexation of $Fe^{III}$ with poly(ethylene glycol) (PEG) and hyaluronic acid functionalized with catechol moieties.[7,39,40] The versatility and tunable properties of MPNs, coupled with their straightforward and robust synthesis methodology, have spurned the development of MPNs and the exploration of their potential use in a range of applications.

2.2. Procedure

The different steps involved in the large-scale synthesis of Fe-TA MPN capsules are detailed below and also shown in Movie S1.

2.2.1. Materials

Iron(III) chloride hexahydrate ($FeCl_3 \cdot 6H_2O$), TA, 3-(N-morpholino)propanesulfonic acid (MOPS), sodium hydroxide (NaOH), tetrahydrofuran (THF), and PS particles (3.55 µm diameter, 10% w/w water suspension, microParticles GmbH) were purchased from standard chemical suppliers (e.g., Sigma-Aldrich) unless stated otherwise. Water with a resistivity of 18.2 MΩ $cm^{-1}$ (Milli-Q water) was obtained from a Millipore Synergy® water purification system and used in all experiments.

2.2.2. Preparation of Solutions

Solutions are prepared as follows. A 37 mM $FeCl_3$ solution is prepared by dissolving 500 mg of $FeCl_3 \cdot 6H_2O$ in 50 mL Milli-Q water. A 24 mM TA solution is prepared by dissolving 2000 mg of TA in 50 mL Milli-Q water. A 1.0 M NaOH solution is prepared by dissolving 2000 mg of NaOH pellets in 50 mL Milli-Q water. MOPS pH 7.4 buffer (20 mM) is prepared by dissolving 209 mg of MOPS in 40 mL Milli-Q water, followed by solution pH adjustment to 7.4 using 1.0 M NaOH solution and topping up to a final volume of 50 mL with Milli-Q water.

**NOTE:** Both $FeCl_3$ and TA solutions should be prepared fresh before use and the MOPS buffer solution should be filter-sterilized with a 0.22 µm filter (Millex-GP syringe filter unit, 0.22 µm pore size, polyethersulfone, 33 mm diameter, Millipore) to prolong storage life.

2.2.3. Washing of PS Particle Templates

To wash the PS particles, 22.5 mL Milli-Q water is added to 2.25 mL of PS particle suspension (10% w/v) in a 50 mL Falcon® tube, and the resulting suspension is thoroughly mixed by vortexing (LSM™ vortex mixer, Corning Inc.) for 1 min and ultrasonication for 1 min. The dispersion is then centrifuged (2500 *g*, 20 min) to pellet the particles (Figure 2a) and 22.5 mL of the supernatant is carefully withdrawn (by pipetting). Removal of this precise volume of supernatant is essential to ensure that subsequent reagent additions yield the desired concentrations. The steps are repeated to perform a second washing.

2.2.4. Assembly of MPNs

Prior to MPN assembly, a volume of 2.25 mL of each $FeCl_3$ and TA solution is pipetted and 22.5 mL of the MOPS buffer is measured. This step ensures that assembly is performed in a timely and efficient manner. The washed particles are resuspended by adding 19.8 mL Milli-Q water, followed by vortexing thoroughly for 1 min. The speed of the vortex mixer is reduced accordingly so that the particle suspension can be mixed/agitated without spilling over. Then, while vortexing, 2.25 mL of the TA solution is added, and the mixture is vortexed at maximum speed for 15 s.

The $FeCl_3$ solution (2.25 mL) is then added using the same methodology as for the TA solution. Successful MPN formation is indicated by the appearance of a milky blue suspension, as shown in Figure 2b. The vortex speed is reduced to allow for mixing without spilling, followed by addition of 22.5 mL MOPS buffer to raise the pH to ~7, after which the lid is closed, and the resulting mixture is vortexed for 60 s at maximum speed. The suspension will turn dark blue/violet (Figure 2c).

2.2.5. Washing of MPN-Coated Particles

The MPN-coated particles in solution are centrifuged (2500 *g*, 20 min) and ~15–19 mL of the supernatant is removed, leaving a small volume in the tube for redispersion. The pellet is re-dispersed by vortexing before 20 mL Milli-Q water is added and the pellet-containing solution is further vortexed for 30 s. The washing steps are repeated a further two times.

**NOTE:** It is important to transfer the particle suspension to a new 50 mL Falcon® tube before commencing the second wash (this is done after the pellet obtained via centrifugation following the first washing cycle is re-dispersed by vortexing). This will help improve the quality of the particles by removing excess material that may have adhered to the tube wall, while also reducing the likelihood of particle agglomeration, as displayed in Figure 3a and 3b.

2.2.6. Dissolution of PS Particle Templates

For dissolution of the template, the MPN-coated particles in solution are centrifuged (2500 *g*, 20 min) and the supernatant is discarded, leaving ~1 mL of solution to allow for subsequent dispersion of the particles by pipetting. THF

(20 mL) is then added and the particles are resuspended through repeated pipetting with a 5 mL pipette (30×). The dissolution step is repeated four times.

**NOTE:** The particles can be incubated on a spinning wheel for 1–2 h during the fifth washing step to remove residual PS core template. Scanning electron microscopy (SEM) and transmission electron microscopy (TEM) can be used to confirm removal of the PS core template, as shown in Figure 4b.

2.2.7. Washing of MPN Capsules

Following dissolution of the PS template, the MPN capsules in THF are centrifuged (2500 *g*, 20 min) (Figure 2d) and ~19 mL of the supernatant is discarded. The pellet is re-dispersed by intermittent pipetting, before 20 mL Milli-Q water is added and the suspension is gently washed through repeated pipetting with a 5 mL pipette (30×) before centrifugation (2500 *g*, 20 min). The supernatant removal, re-dispersion, washing, and centrifugation steps are repeated to wash the capsules a second time. The capsules are then resuspended in 13.5 mL Milli-Q water (Figure 2e).

**NOTE:** MPN capsules should be stored on a wheel or similarly kept in motion to prevent agglomeration and/or sedimentation.

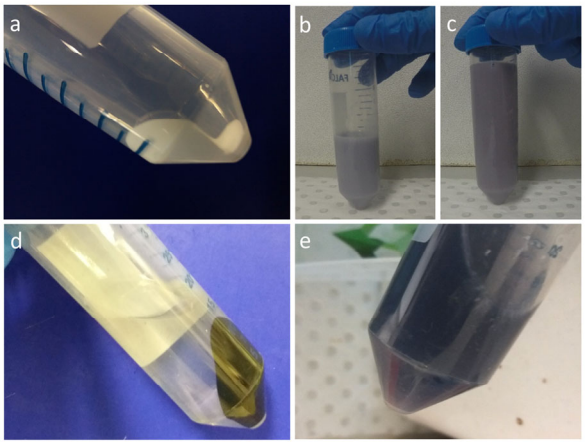


**Figure 2.** Photographs showing the various steps involved in the discrete assembly of Fe-TA MPNs: (a) PS particle pellet following washing and centrifugation; (b) MPN-coated PS particles in solution following addition of $Fe^{III}$ and TA; (c) MPN-coated PS particles in solution following addition of MOPS buffer; (d) MPN capsule pellet following PS template dissolution and centrifugation; and (e) MPN capsules dispersed in water.

2.3. Challenges and Considerations

Figure 4 and Table 1 summarize the properties of the synthesized Fe-TA MPN capsules. A yield of ~74 mg of the Fe-TA MPN capsules per Falcon tube (50 mL) was obtained, resulting in ~444 mg for a sequence of six tubes, and a potential yield of just under 1 g when performing the synthesis with two parallel sets of 6 Falcon® tubes. This is a significant increase when compared with smaller-scale yields of ~0.16 mg per (15 mL) tube. The TEM images confirm successful MPN coating of the PS particle templates (Figure 4a), while also exhibiting the typical profile of a collapsed MPN capsule following dissolution of the PS template (Figure 4b). A capsule diameter of 3.5 ± 0.4 µm was observed using TEM. The atomic force microscopy (AFM) image and height profile (Figures 4c and 4d, respectively) displayed an identical collapsed (air-dried) MPN capsule profile to that observed with TEM, with a measured Fe-TA MPN capsule diameter of 3.7 ± 0.3 µm and thickness of 11.2 ± 1.2 nm. The shape profile and dimensions are in good correlation with their smaller-scale synthesized Fe-TA MPN equivalent values reported by Ejima et al.[31] The average zeta potential value of the Fe-TA MPN capsules prepared from our large-scale synthesis protocol was slightly less negative (−59 ± 10 mV) than that observed by Ejima et al. (−65 ± 7 mV)[31] but within the standard deviation. The UV–vis absorbance spectrum of the Fe-TA MPN (Figure 4e) showed a similar profile to that reported by Ejima et al.[31] In particular, the presence of the ligand-to-metal charge transfer (LMCT) band at ~520 nm was visible, indicating coordination between $Fe^{III}$ and TA.[41] This band was absent in the spectrum of TA. Finally, the Fourier transform infrared (FTIR) spectrum of the large-scale Fe-TA MPN (Figure 4f) displayed a similar profile to that reported by Guo et al.[12] The presence of a new band at ~1270 $cm^{-1}$ in the Fe-TA spectrum is indicative of coordination between Fe and TA, while the reduced intensity and relatively flat and broad peak at ~3500 $cm^{-1}$ (assigned to –OH stretching) suggests fewer unoccupied hydroxyl groups on TA due to coordination. These results strongly indicate that MPN formation was successful, and that the MPNs displayed similar dimensions and properties to their smaller-scale equivalents as documented in the scientific literature, thus validating our current large-scale synthesis protocol.

Discrete assembly of MPNs onto templates has been extensively studied, using a range of templates and metal–ligand combinations.[32–34] Similarly, the influence of compositional variables (metal-to-ligand ratio and concentration, substituent choice and size, reaction media pH) on MPN formation and particle/capsule properties has been thoroughly investigated.[12,42,43] These parameters apply when synthesizing MPNs at increased volumes and as such will not be discussed in this section. In addition, although multiple assembly steps (using alternating coating/washing cycles of metal ions and polyphenols) result in MPN capsules with different properties than counterparts prepared via a single-step technique[36,44] (such as that discussed in this section), the techniques and equipment used for potential large-scale synthesis are identical. The primary considerations and challenges associated with the large-scale discrete assembly of MPNs arise during the template and specimen washing steps, i.e., centrifugation, supernatant removal following pelletization, and mixing/redispersion as detailed below and summarized in Table 2.

*(i) Template and Specimen Pelletization via Centrifugation*

To remove the supernatant during multiple washing iterations, centrifugation is generally used to pelletize the particle/capsule prior to adding fresh solvent. As with smaller, bench-top scale syntheses, similar considerations and challenges apply at increased volumes. First, selecting appropriate centrifugation speeds and times is essential to reducing the likelihood of particle/capsule aggregation and/or insufficient pelletization. The centrifugation speeds and times are dependent on particle diameter, with faster speeds and longer times typically required as particle diameter decreases. Ideally, the lowest possible speed and time required to result in a pellet with minimal particles remaining in the supernatant would be used, with a clear supernatant following

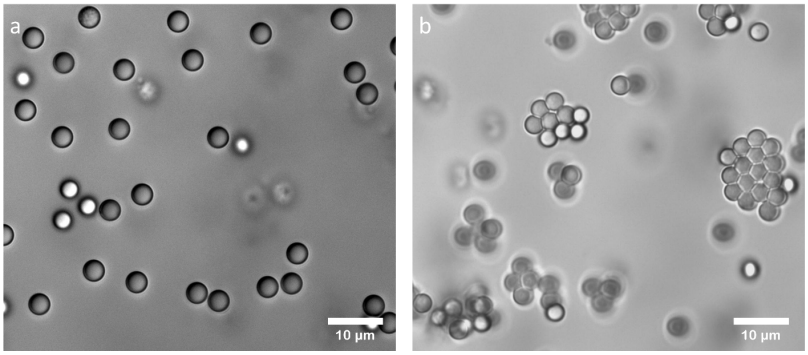


**Figure 3.** Differential interference contrast microscopy images of (a) non-agglomerated and (b) agglomerated MPN-coated PS particles in aqueous solution.

centrifugation being the measure of a successful process. It is important that this "critical" speed is not exceeded, as the likelihood of particle agglomeration increases with centrifugation speed. A detailed guide correlating centrifugation speeds and times with particle diameter published by Björnmalm et al.[29] was used as an initial guide for the present study. The speed and times used therein[29] were optimized and suitable for 2 mL centrifuge tubes but inappropriate when larger (50 mL) Falcon® centrifugation tubes were involved. Initial trials using 50 mL tubes resulted in a cloudy supernatant and partially pelletized specimens, highlighting that direct scaling and translation of experimental parameters are seldom successful at increased scales. For the present study, centrifuging at 2500 *g* for 20 min successfully produced pelletized specimens, with no aggregation, and a clear supernatant. These settings were applied for the 3.55 µm PS templates and MPN-coated PS particles.

In addition to the centrifugation time and speed, the volume of solvent and concentration of templates/particles and capsules within a tube need to be considered. Increasing solvent volumes and concentrations leads to particle deposition along the swinging bucket rotor wall, resulting in a loosely packed stream of particulate rather than a pellet centered at the base of the rotor.[29] This can influence the yield as the likelihood of particles remaining suspended throughout the supernatant increases with increasing particle concentration. Inaccuracies in yield control can be further exacerbated during supernatant removal, with turbulence during liquid removal disturbing the material deposited on the rotor wall. To minimize these occurrences, a maximum volume of ~42 mL was used within each 50 mL Falcon® tube. Pelletized specimen formation was restricted to the base of the tube, with little-to-no deposition on the tube wall evident.

*(ii) Supernatant Removal*

The precise and careful removal of a small volume of supernatant noted in the procedure by Björnmalm et al.[29] is essential to ensure that the pellet is not disturbed, thus maximizing product yield. This is especially important for PS template washing, PS dissolution in THF, and MPN capsule washing, whereas when washing MPN-coated PS particles, the supernatant can be removed by tilting the tube rather than pipetting. At increased scales, this precision is as important, particularly if manual pipetting is performed. As mentioned in *Template and Specimen Pelletization via Centrifugation*, ensuring the formation of a solid pellet at the base of the tube, with little-to-no particle deposition on the tube wall reduces the likelihood of removal of both the product and supernatant. However, challenges can still present themselves despite successful pelletization. The sheer volume of supernatant used in the present study is generally beyond the range of pipetting volumes used in most academic laboratories (with 5 mL typically being the largest volume), thereby necessitating repeated pipetting from the same tube to remove the desired amount of liquid. Such a procedure presents ergonomic and time constraints, as well as increasing the likelihood of disturbing the pellet with each pipetting event. If one considers the maximum potential capacity of a centrifuge (in the case of the present study, six Falcon® tubes each containing a maximum volume of ~42 mL liquid), the demands on the researcher are significantly increased. These demands are further aggregated if one considers that the experiments can be performed in duplicate to maximize yields, with one series of 6 × 50 mL tubes undergoing pelletization while washing/redispersion is being conducted on a second series of tubes.

There are various strategies that can be employed to either reduce or eliminate these aforementioned challenges and increase yield recovery. The simplest approach would be to use larger-volume (i.e., 10 or 20 mL) pipettes although they would still require care and attention to the task at hand, with the risk of particle disturbance still present. Another option would be the use of tube holders that angle the tube at a degree for comfortable and ergonomic pipetting, without obscuring the view inside the tube. Ideally, the use of vacuum-controlled pipettes would be the most readily adaptable option for most academic laboratories. Otherwise, automated pipetting machines, possibly coupled with automated centrifugation, would provide the most consistent and least-demanding option in terms of human resources.

*(iii) Particle Redispersion*

In the literature, bench-top vortex mixing and ultrasonic bath immersion have been used for particulate redispersion and washing for a range MPNs and these were similarly employed using 50 mL Falcon® tubes in the present study. Sufficient mixing/shear efficiency was obtained, with effective dispersion of PS templates, MPN-coated PS, and MPN capsules at increased loadings. To accommodate the larger tube volumes, we recommended that the tubes are moved across the vortex mixing head to prevent potential "dead spots", which would not be subject to agitation, and to promote thorough dispersion. Additionally, overfilling of the Falcon® tubes is not advised, as the addition of solvent under vortexing can result in spillage and potential yield loss (a maximum volume of ~42 mL was used in the present study).

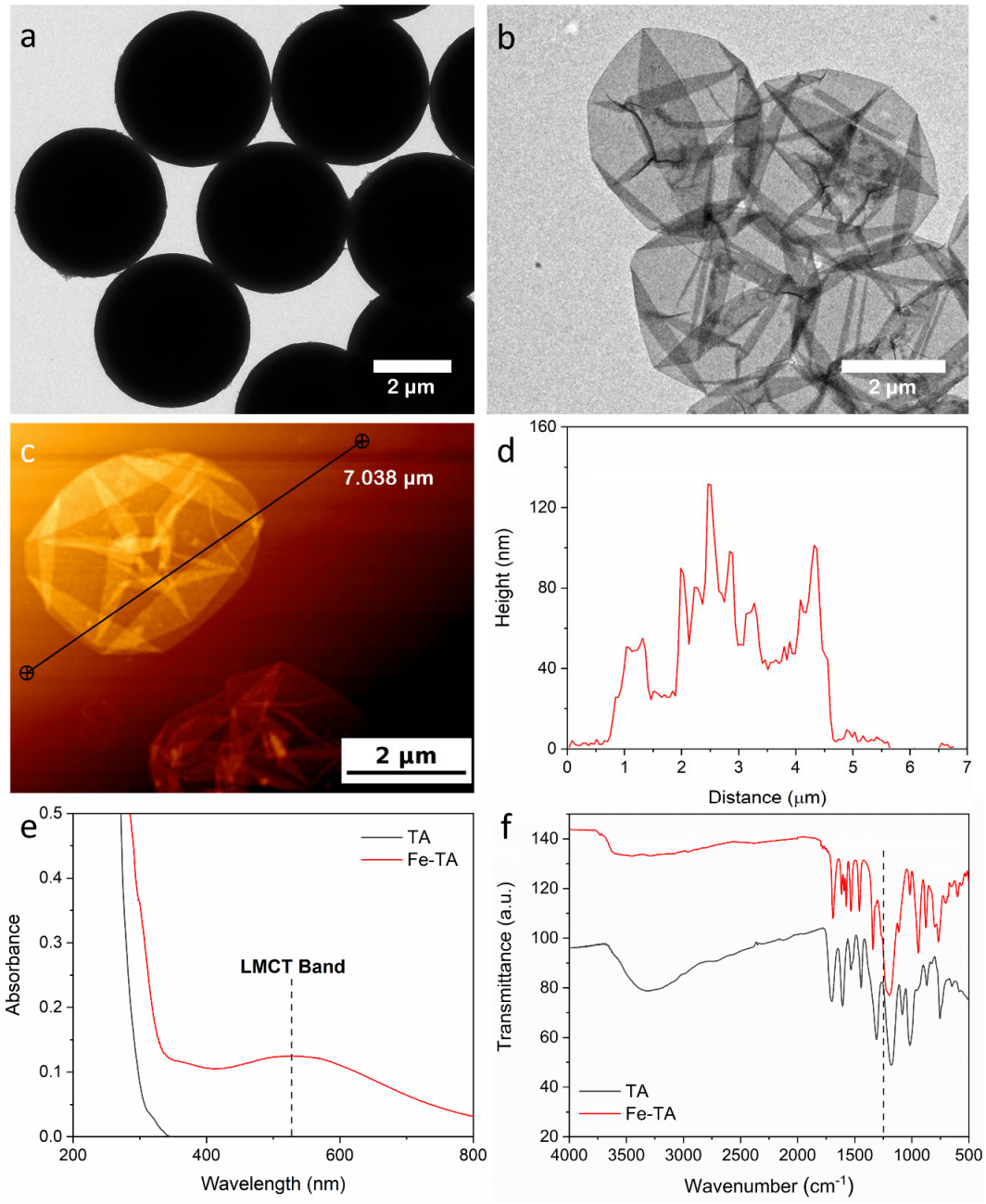


**Figure 4.** TEM images of (a) Fe-TA MPN-coated PS particles and (b) Fe-TA MPN capsules prepared via direct assembly. (c) AFM image and (d) corresponding height profile of Fe-TA MPN capsules. (e) UV–vis spectra of TA and Fe-TA MPN capsules in solution at pH 8.0. (f) FTIR spectra of TA and Fe-TA MPN capsules.

**Table 1. Comparison of large-scale experimental data and laboratory-scale reference data for Fe-TA MPNs prepared via discrete assembly**

| Property | Large-scale experimental data | Laboratory-scale reference data[a] |
|---|---|---|
| Yield | ~74 mg per tube | ~0.16 mg per tube[b] |
| Diameter (TEM) | 3.5 ± 0.4 µm | ≈3.6 µm |
| Diameter (AFM) | 3.7 ± 0.3 µm | ≈3.6 µm |
| Thickness (AFM) | 11.2 ± 1.2 nm | 10.4 ± 0.6 nm |
| Zeta potential | −59 ± 10 mV | −65 ± 7 mV |

[a]The reference data were obtained from Ejima et al.[31] Spherical PS templates with a diameter of 3.55 µm were coated with MPNs.

[b]Yield data were not reported in Ejima et al.[31] Thus, the experiments were replicated and the yield was determined gravimetrically.

**Table 2. Key considerations and challenges for the reproducible, large-scale synthesis of Fe-TA MPN capsules via discrete assembly onto PS templates; E-MPN capsules via interfacial self-assembly on oil-in-water emulsions; and Si-SPs via gel-mediated electrospraying assembly**

| Capsule/particle system | Key considerations and challenges | Details |
|---|---|---|
| Fe-TA MPN capsules via discrete assembly | *Centrifugation:* Speed and time must be selected to ensure pelletization without agglomeration, while trying to use the minimal centrifugation time possible. | Falcon® tubes (50 mL) filled with a maximum volume of ~42 mL were used. Centrifugation conditions were 2500 *g* for 20 min (specific for 3.55 µm PS templates). |
| | *Supernatant removal:* Disturbing the pellet during supernatant removal can reduce the MPN-coated particle/capsule yield. | Care must be taken during manual pipetting. Ergonomic aids (e.g., tube holders, larger manual pipettes or vacuum-controlled pipetting devices) and automation can help improve precision. |
| | *Particle redispersion:* Sufficient mixing/shear efficiency must be employed to ensure particle/capsule redispersion at increased volumes | Falcon® tubes should be moved across the vortex mixing head to promote thorough dispersion and prevent the formation of "dead spots". Tubes should not be overfilled to prevent spillage/yield loss. |
| E-MPN capsules via interfacial self-assembly | *Oil/water emulsion stability:* Emulsion concentrations of up to 0.3% v/v are stable for only a few hours. | Emulsions should be prepared fresh and used promptly for the synthesis E-MPNs. Emulsification using an ultrasonicator with a microtip was successful. Microfluidic and flash nanoprecipitation/nanocomplexation techniques or the addition of stabilizers may promote emulsion longevity, though these options must be investigated. |
| | *E-MPN filtration:* Small column volumes, ligand compatibility with the stationary phase, manual monitoring of color changes, meniscus levels and starting/stopping E-MPN capsule collection present challenges for maximizing yield. | Care and patience must be taken during filtration. Automation and robotics (e.g., the use of pumps to add liquid to the column, optical controllers to distinguish between sample and washing liquid) is one such proposal. Chromatography or similar column-based methods may provide a continuous, high-throughput filtration and collection method. |
| Si-SPs via gel-mediated electrospraying assembly | *Dispersion of primary silica particles in alginate solution:* Dispersion/ultrasonication efficiency can decrease at increased silica/alginate volumes, leading to agglomeration. | Using larger tubes that are not completely filled with particles/alginate solution or preparing several smaller (e.g., 15 mL) tubes in series can mitigate the chance of particle agglomeration at increased volumes. |
| | *Electrospraying device configuration:* Experimental variables and conditions must be controlled to ensure reproducibility. Deviations can influence the shape and size homogeneity of the Si-SPs. | A sealed chamber to house the electrospraying assembly was used to control the environment and prevent external anomalies. The tubing and needle must be completely charged with the primary silica particles/alginate solution and free of air pockets prior to switching on the pump to prevent flow irregularities/sputtering. Needle orientation should be as perpendicular to the bench surface as possible to encourage the formation of spherical SPs. Wires contacted the nozzle and gelling bath at identical points every time the setup was used and the number of conductive materials within the chamber was kept to a minimum to promote consistent voltage difference. |
| | *SP harvesting, washing, and calcination:* Alginate/Si-SPs are gel-like and easily deformed by manual handling or excessive force during washing. SPs can fuse during calcination if in contact with one another and can migrate during calcination if not placed on a flat/even section of the porcelain dish. Calcined SPs are delicate and can crack/chip. | A plastic Pasteur pipette with the tip cut at the point where it begins to narrow was used to remove the alginate/Si-SPs. A gentle touch and patience are essential when handling alginate/Si-SPs. Gentle rocking during SP washing is also necessary to prevent deformation; this can be performed manually or mechanically. A pipette tip was used to gently separate alginate/Si-SPs to ensure that they are not in contact with each other or touching the curved walls of the porcelain dish. Gentle handling of calcined Si-SPs (i.e., gently moving particles with a pipette tip when required) was performed. |
| | *Time considerations:* Larger-scale fabrication of SPs involves increased time and human resource demands, along with process monitoring. | Effective planning, time management, and sharing of workload can help mitigate time-related issues. The ability to stop and re-start the electrospraying process at a later point in time provides the greatest degree of flexibility. |

Alternative dispersion/mixing techniques, involving magnetic stirring plates and mechanical stirrers, have been investigated at similar increased volumes, with initial results showing successful dispersion of templates and capsules, without excessive agglomeration. An investigation is underway to determine whether the extent of dispersion using these aforementioned techniques is as effective as with vortex mixing. Successful implementation of these may remove the restrictions on sample volume imparted by Falcon® or similar tubes.

*(iv) Method Automation Considerations*

A range of automated devices and systems have been used for the discrete assembly of MPNs albeit at laboratory scale yields.[44–49] However, the reduced human resource requirements and the possibility of continuous throughput encourage their use for large-scale, high-throughput MPN production. Commercial and custom-built robotic dippers have been used to coat spherical and planar substrates, with the option of controlling incubation time, number of coating cycles, temperature, and pH.[45,46] Microfluidics has been exploited to prepare micro- and nanoparticles,[47–49] with the possibility of coating solutions, particle templates, and washing solution being fed into the system. Multi-channel setups allow for numerous coating iterations and control of particle flow relative to the coating and washing streams. Similarly, flash nanoprecipitation and flash nanocomplexation are an emerging class of techniques, in which particle formation is instigated by the turbulent mixing of two or more oppositely charged polyelectrolyte solutions within a multi-inlet vortex chamber.[50] Continuous high-throughput synthesis of reproducible particles, enhanced process control and increased drug loading, encapsulation efficiency and bioactivity retention of proteins have been reported for particles prepared using flash nanocomplexation,[50] presenting the potential to synthesize MPNs using this technique.

## 3. INTERFACIAL SELF-ASSEMBLY OF MPNs ONTO OIL/WATER EMULSIONS

### 3.1. Overview

Template-mediated self-assembly has been used to prepare a range of engineered systems suitable for drug delivery, including capsules[1,51] and liposomes.[52] As with many particle synthesis techniques, material properties are determined by the choice of reagents, as well as the shape of the template, with various solid,[53,54] porous,[55,56] and liquid[57,58] templates being employed. The choice of template can also influence the loading of therapeutics, with oil/water emulsion templates allowing hydrophobic moieties to dissolve within the oil phase.[59] Furthermore, the surface chemistry of the fabricated particles determines interactions with biomolecules, while also dictating the behavior of the materials in vivo.[49] A particularly interesting family of macromolecules are PEG derivatives, which can readily attach to the surface of nanoparticles.[60] Increased blood circulation time, low-fouling, and stealth-like behaviors have been introduced to nanoparticles via the presence of PEG-based surface moieties. The formation and purification of self-assembled Fe-PEG-polyphenol MPNs using oil/water emulsion templates, referred to as E-MPNs, have been successfully demonstrated (Figure 5)[7] via a robust, reproducible, and relatively simple methodology. The E-MPNs successfully internalized in cells and served as a drug delivery vehicle, in addition to exhibiting low-fowling behavior and a pH-triggered decomposition profile. These PEG-based MPNs prepared using emulsion templates show potential in facilitating the selective targeting and release of large loadings of therapeutic molecules.

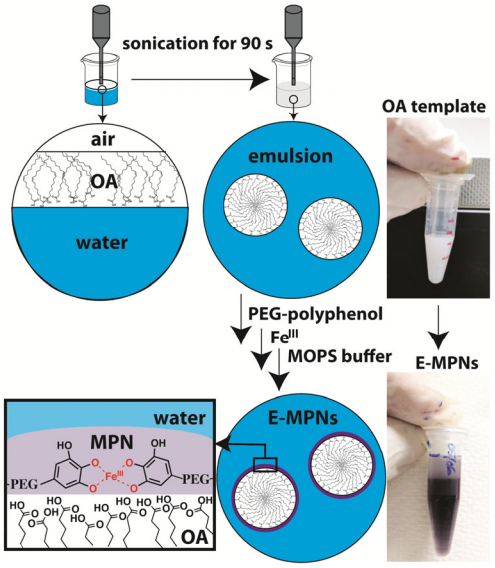


**Figure 5.** Overview of the preparation of oil/water emulsion templates and subsequent self-assembly of Fe-PEG-polyphenol MPNs on their surface. OA, oleic acid. Reproduced with permission from reference.[7] Copyright 2018 WILEY-VCH Verlag GmbH & Co.

### 3.2. Procedure

The large-scale synthesis protocol used to prepare E-MPNs is detailed below and summarized in Movie S2.

#### 3.2.1. Materials

PEG-polyphenol (5-hydroxydopamine-modified 8-arm-PEG-syccinimidyl succinate, synthesized as detailed therein[7] and frozen in water), oleic acid (OA), $FeCl_3 \cdot 6H_2O$, Dulbecco's phosphate-buffered saline (DPBS), MOPS, ethanol, and anhydrous dimethyl sulfoxide (DMSO) were purchased from standard chemical suppliers (e.g., Sigma-Aldrich) unless stated otherwise. Milli-Q water with a resistivity of 18.2 MΩ $cm^{-1}$ was used in all experiments.

#### 3.2.2. Preparation of Solutions

Solutions are prepared as follows: A 24 mM $FeCl_3$ solution is prepared by dissolving 330 mg of $FeCl_3 \cdot 6H_2O$ in 50 mL Milli-Q water. MOPS pH 8.0 buffer (10 mM) is prepared by dissolving 210 mg of MOPS in 80 mL Milli-Q water, followed by solution pH adjustment to 8.0 using 1.0 M NaOH solution and topping up to a final volume of 100 mL with Milli-Q water. The $FeCl_3$ solution should be freshly prepared before use.

#### 3.2.3. Preparation of Nano-Emulsion (Oil/Water Emulsion Template)

In a 50 mL Falcon® tube, 16.5 mL Milli-Q water and 4.5 µL OA are added. The ultrasonic probe tip (Qsonica® S-4000 with XL2000 microprobe) is placed between the 6–10 mL mark on the tube and the content of the tube is sonicated at an amplitude of 40% for 1 min. The tube is then placed in a fridge for 20 min to cool (cooling reduces Brownian motion which can instigate Ostwald ripening). The cooled emulsion is then loaded in a 20 mL syringe and filtered through a 0.22 µm membrane filter into a 50 mL Falcon® tube. The diameter of

the nano-emulsion can be measured via dynamic light scattering (DLS).

3.2.4. Coating of Nano-Emulsions with MPNs (E-MPNs)

For MPN coating of the nano-emulsions, 1.65 mL of the nano-emulsion is introduced into a 15 mL Falcon® tube (Figure 6a) followed by the addition of 825 µL of PEG-polyphenol (20 mg $mL^{-1}$) solution under gentle vortexing. The vortex speed is subsequently increased and applied for 30 s (Figure 6b). The PEG-polyphenol was thawed at room temperature for at least 20 min prior to use. The emulsion is rotated on a wheel for 15–20 min to allow PEG-polyphenol assembly at the oil–water interface of the emulsions. The Falcon® tube is removed from the rotating wheel and subsequently placed on a vortex mixer at reduced speed with the cap of the tube removed and the tube held gently to the side to prevent spilling. Then, 584 µL of the $FeCl_3$ solution (Figure 6c) is added to the tube while vortexing, followed by 4 mL of MOPS buffer (10 mM, pH 8.0) (Figure 6d).

**NOTE:** The addition of excess PEG-polyphenol is required to completely cover the emulsion surface. Following the coating process with final addition of MOPS buffer, the color of the solution should turn dark purple/black (Figure 6d), indicative of successful complexation.

3.2.5. Purification of E-MPNs

An illustra™ NAP-25 Sephadex® (GE Healthcare, Life Sciences) column is set up with a small glass bottle placed underneath. The caps at the base and top of the column are removed, after which the column buffer begins dripping into the bottle. At least 3 mL of DPBS is introduced into the column to wash the column and attain a pH of ~7.4. When the meniscus of the DPBS is on top of the stationary phase within the column, the MPN solution is introduced in the column. DPBS (3 mL) is subsequently introduced when the meniscus of the MPN solution is on top of the stationary phase within the column (to prevent dilution).

**NOTE:** It is advised to add the DPBS dropwise (5–10 drops) using a Pasteur pipette and wait for a few seconds before addition of another 5–10 drops. The remainder of DPBS can then be added. The resulting dark fraction (Figure 6e) is then collected (~2–4 mL). The more transparent the collected fraction is, the more diluted the MPN solution is. The use of a white tile or piece of paper placed below the collection vessel is recommended to assist with the visualization of changes in color. To purify another aliquot, the column is washed with at least 3 mL of DPBS before addition of the sample. The column can be re-used on the same day if it does not run dry.

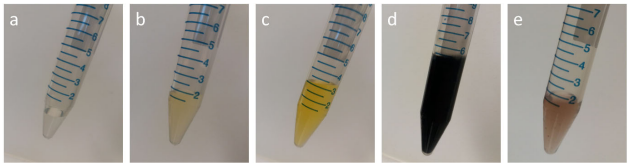


**Figure 6.** Photographs showing the various steps involved in the self-assembly of E-MPNs onto oil/water emulsions: (a) the filtered oil–water nano-emulsion; MPN-coated emulsion following sequential additions of (b) PEG-polyphenol, (c) $FeCl_3$ solution, and (d) MOPS buffer; and (e) the purified E-MPNs following filtration.

3.3. Challenges and Considerations

The properties of the E-MPNs and oil/water emulsion are summarized in Figure 7 and Table 3. Approximately 100 µg of E-MPNs was obtained per tube, which demonstrated scalability from the yield (~51 µg) obtained at smaller scales. Despite the two-fold increase in yield obtained from a single Falcon® tube, conducting E-MPN fabrication with a series of tubes could be used to further increase the amount of E-MPNs obtained. The method could further be scaled using increased amounts of reagents and larger vessels; however, the success of synthesis at these increased scales will be subject to ensuring that sufficient ultrasonication is achieved to facilitate formation of the oil/water emulsion in addition to sufficient mixing during E-MPN formation (as required for MPNs fabricated on PS templates). Emulsion formation and stability will be expanded on in the following section.

As observed from the TEM images in Figure 7a and 7b, the E-MPNs displayed a typical circular structure with an average diameter of 195 ± 81 nm; the large variation in size of the E-MPNs was also observed by Besford et al.[7] Similarly, the AFM image and accompanying height profile (Figure 7c and 7d, respectively) show the spherical morphology of the E-MPNs, with an average diameter of ~190 nm; the diameter measured via DLS was slightly lower at 174 ± 85 nm (Figure 7e). The experimental E-MPN diameter values were slightly lower than those reported by Besford et al. (200 nm, as measured by AFM, and 180 ± 70 nm, as measured by DLS).[7] In contrast, the DLS-derived average diameter of the oil/water emulsion (163 ± 68 nm) was slightly higher than that reported by Besford et al. (150 ± 58 nm).[7] However, the diameters of both the E-MPNs and oil/water emulsion prepared using the current protocol fell within standard deviation values, although it should be noted that significant deviations are present within our experimental data and that of Besford et al.[7] The average zeta potential value of E-MPNs was −9 ± 4 mV, comparable with that reported by Besford et al. (−10 mV),[7] and that of the oil/water emulsion was −35 ± 9 mV, the same (within error) as that (−45 mV) reported by Besford et al.[7] However, both sets of zeta potential values are low, suggesting a similar degree of low E-MPN stability. The UV–vis absorbance spectra of the PEG-polyphenol, oil/water emulsion, and E-MPN are presented in Figure 7f. The spectra showed similar profiles to those presented by Besford et al.[7] Most notably, the E-MPN spectrum displayed an additional band at ~520 nm, which corresponds to the LMCT band, indicating coordination between $Fe^{III}$ and PEG-polyphenol. These results are consistent with those reported in literature, indicating that the large-scale protocol developed herein can successfully replicate E-MPNs with similar property profiles. Some of the main challenges and further considerations are detailed below and summarized in Table 2.

*(i) Oil/Water Emulsion Stability*

The concentration of OA in water was 0.03% v/v, which yielded emulsions of ~160 nm in diameter (Figure 7e). Besford et al.[7] reported that concentrations of up to 0.3% v/v could be used to prepare stable emulsions; however, uncoated emulsions were only stable for several hours before they begin to aggregate (in contrast to E-MPNs that remain stable for up to 9 days). Thus, the first consideration is the limited timescale within which the emulsions can be used as templates. The emulsion (16.5 mL) prepared in the present study, which is adequate for producing a significant yield of MPNs, is thus expected to have a shelf-life of several hours before

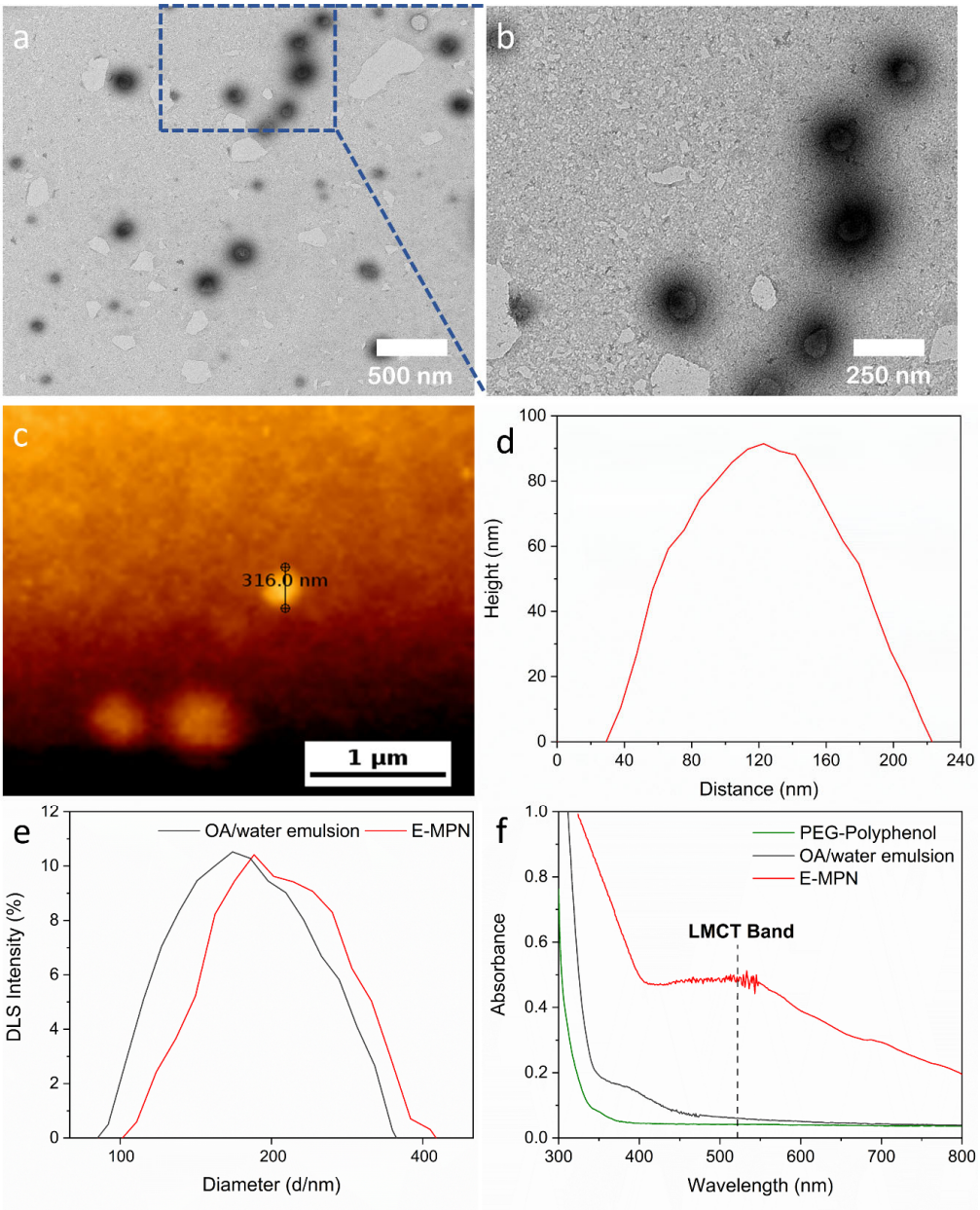


**Figure 7.** TEM images of E-MPN capsules at (a) low and (b) high magnification; (b) is a high-magnification image of the area encased in blue in (a). (c) AFM image and (d) accompanying height profile of E-MPN capsules. (e) DLS size distribution of E-MPN capsules and OA/water emulsion. (f) UV–Vis absorption spectra of OA/water emulsion, E-MPN, and PEG-polyphenol.

**Table 3. Comparison of large-scale experimental data and laboratory-scale reference data for E-MPNs (Fe-PEG-Polyphenol MPNs) prepared via self-assembly on oil/water emulsions**

| Property | Large-scale experimental data | | Laboratory-scale reference data[a] | |
|---|---|---|---|---|
| | Emulsion | E-MPN | Emulsion | E-MPN |
| Yield | 16.5 mL | ~100 µg per tube | 5 mL | ~51 µg per tube[b] |
| Diameter (AFM) | – | ≈190 nm | – | ≈200 nm |
| Diameter (DLS) | 163 ± 68 nm | 174 ± 85 nm | 150 ± 58 nm | 180 ± 70 nm |
| Diameter (TEM) | – | 195 nm ± 81 nm | – | ≈200 nm |
| Zeta potential | −35 ± 9 mV | −9 ± 4 mV | −45 mV | −10 mV |

[a]The reference data were obtained from Besford et al.[7]

[b]Yield data were not reported in Besford et al.[7] Thus, the experiments were replicated and the yield was determined gravimetrically.

agglomeration. Although the relatively fast speed at which MPN formation occurs using the current protocol facilitates a high yield and throughput of MPN-coated emulsions, alternative methods to increase stability (e.g., addition of stabilizing agents, use of high-pressure homogenization or similar techniques for stable emulsion formation[61]) should be considered. However, the influence of additives on MPN formation and stability must also be investigated and considered. If larger volumes of emulsion are prepared, the emulsification efficiency of ultrasonic probes (and other shear-based emulsification devices) at increased volumes needs to be considered, which may limit the amount of emulsion that can be prepared. The potential variation in emulsification performance between devices with varying capacities and operational principles is another factor that requires further investigation. The use of microfluidics and flash nanoprecipitation/nanocomplexation for the discrete assembly of MPNs[47–50] may also be applied for emulsion preparation (as well as the self-assembly of MPNs onto emulsions), which may potentially reduce or eliminate challenges concerning limited emulsion stability. Despite these considerations, the data confirmed that the use of an ultrasonicator with a microtip probe successfully yielded oil/water emulsions with diameters of ~160 nm (Figure 7e).

*(ii) E-MPN Filtration*

Aside from the time constraints imparted by emulsion stability, the MPN filtration process is a second consideration. The limited capacity of the 2.5 mL Sephadex® column used, as well as the need to manually monitor solvent levels, color changes to commence/stop E-MPN capsule collection and addition of the MPN-coated emulsion and DPBS washing solution presents a significant time and human resources factor. The choice of ligand additionally presents considerations for filtration. The PEG-polyphenol (5-hydroxydopamine-modified 8-arm-PEG-syccinimidyl succinate) used for E-MPNs has a low affinity for silica, thus allowing it to readily pass through the column. In contrast, TA-based MPNs would adhere and block the column owing to the high affinity of TA for silica. Similarly, the risk of excessively diluting the specimens during filtration may eliminate certain purification methodologies (e.g., dialysis). Performing filtration in series, with multiple columns, could be one potential solution, although this would require significant concentration and coordination by the researcher. Automation and robotics could provide a high-throughput and less resource-intensive solution, following calibration and optimization. Pumping and the use of optical controllers to distinguish between sample and washing liquid is one such proposal. Alternatively, chromatography or similar column-based methods may be employed to provide a continuous, high-throughput filtration and collection method.

## 4. GEL-MEDIATED ELECTROSPRAYING ASSEMBLY OF SILICA SUPRAPARTICLES

### 4.1. Overview

The diverse range of properties exhibited by colloidal particles, including but not limited to electronic, magnetic, optical, and catalytic, encourages their potential applicability across a vast array of disciplines.[62–65] Assembly/clustering of colloidal particles results in the formation of SPs, with typical diameters ranging from several micro- to millimeters and property profiles distinct from those of their colloidal precursors.[66,67] Furthermore, the size and shape of the SPs can determine their mechanical and physiochemical properties.[30]

As such, SPs have been applied in diverse fields, including photonics,[68,69] biosensing,[70] catalysis,[71] water remediation,[72] and drug delivery.[73,74] Evaporation-induced self-assembly (EISA)[75] and mold templating[76] have been commonly employed to prepare SPs but require long processing times (generally because of the solvent removal/evaporation step) and significant manual handling by a skilled operator for reproducible synthesis. Recently, gel-mediated electrospraying has been employed to reproducibly produce large volumes of silica SPs (Si-SPs; Figure 8).[30] Primary silica particles are introduced into an alginate solution and the mixture is sprayed through a nozzle—the application of a high voltage to the solution generates a plume of droplets referred to as a Taylor cone.[30] These droplets are collected in a calcium chloride ($CaCl_2$) solution, with the $Ca^{2+}$ ions cross-linking the particle-containing alginate droplets, resulting in the encapsulation of the primary silica particles into gelled beads. Subsequent calcination removes the alginate, yielding Si-SPs. The semi-continuous nature of the methodology presents several advances over the state-of-the-art techniques currently available in the literature, including minimal manual handling, greater approachability, increased throughput and reduced hands-on time (30 min using the current electrospraying technique as opposed to 2 weeks using EISA to generate the same yield), improved variable control, and greater method robustness and reproducibility.

### 4.2. Procedure

The larger-scale synthesis protocol used to prepare Si-SPs is detailed below and summarized in Movie S3. The experimental setup is shown in Figure 9.

#### 4.2.1. Materials

Alginic acid sodium salt from brown algae (alginate), $CaCl_2$, tetraethyl orthosilicate (TEOS), polyacrylic acid (PAA; $M_w$ ~250 kDa, 35 wt.% solution in water), ammonium hydroxide solution (28–30%), ethanol, and cetyltrimethylammonium bromide (CTAB) were purchased from standard chemical suppliers (e.g., Sigma-Aldrich) and used without further purification. Milli-Q water with a resistivity of 18.2 MΩ $cm^{-1}$ was used in all experiments.

#### 4.2.2. Preparation of Primary Silica Particles

The following procedure outlines the synthesis of primary silica particles (~1 μm diameter) with a bimodal porous structure with large pores (15–64 nm) and small pores (2–3 nm) based on the methodology of Ma et al.[30] Commercially available primary particles (including porous and nonporous) can also be used for SP production.

CTAB (2 g) is suspended in 50 mL Milli-Q water at room temperature, followed by the addition of 7.8 g of PAA under vigorous mechanical stirring. After 20 min, a clear solution should be visible, to which 6.36 mL of ammonium hydroxide solution is added, and the solution is stirred for 20 min to yield a milky white solution. TEOS (8.1 mL) is added and the resulting mixture is vigorously stirred for 15 min. The resulting suspension is then placed into a Teflon-lined autoclave at 363 K for 48 h. The silica particles are subsequently retrieved, washed with Milli-Q water and ethanol twice, then dried at 353 K overnight. Finally, the silica particles are calcined in a chamber furnace at 823 K for 30 h

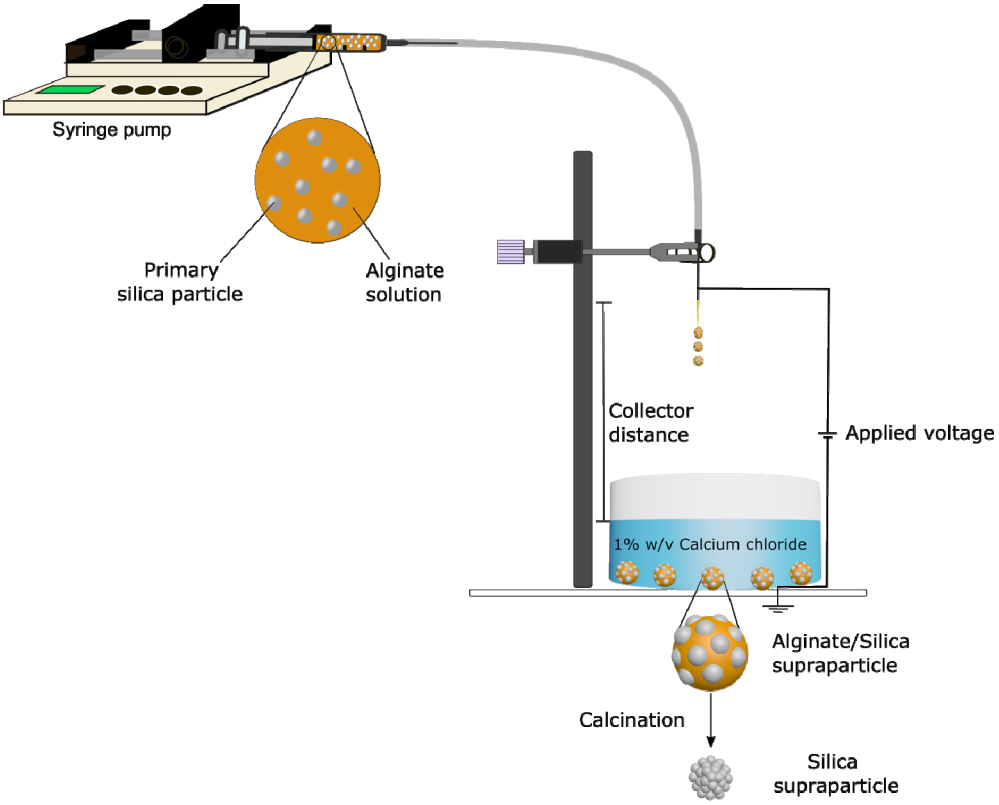


**Figure 8.** Schematic of the setup used for the fabrication of Si-SPs via gel-mediated electrospraying. Reproduced with permission from reference.[30] Copyright American Chemical Society 2018.

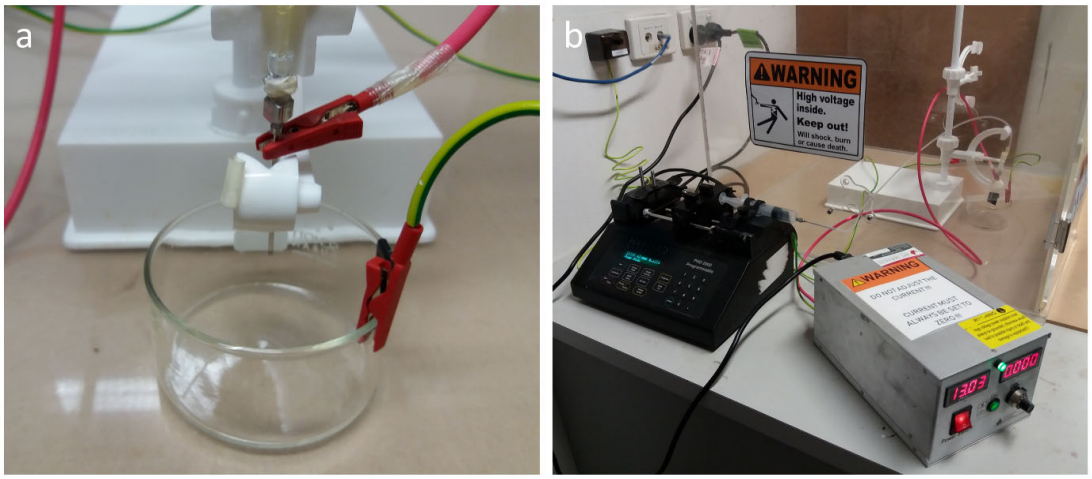


**Figure 9.** Photographs of the electrospraying device setup used for the fabrication of Si-SPs in the present study: (a) extrusion nozzle attached to the high-voltage wire (red wire) and collection dish attached to the earth/return wire (green and yellow wire) and (b) closed chamber prepared for electrospraying with the high-voltage power source and syringe pump located outside the closed chamber.

(heating ramp of 5 K $min^{-1}$) under air to remove any organic material.

4.2.3. Preparation of Primary Silica Particles/Alginate Solution

The synthesized primary silica particles with large pores (diameter of particles ~800 nm, Figure 10a) are first suspended in 20 mL of alginate aqueous solution (30 mg $mL^{-1}$ in Milli-Q water) in a 15 mL Falcon® tube at room temperature to yield a final primary silica particle concentration of 40 mg $mL^{-1}$ within the alginate solution. The suspension is vortexed, ultrasonicated (30% amplitude, 40 s) using an ultrasonic probe, followed by further ultrasonication in a bath for 1 h to achieve an even distribution of the primary silica particles throughout the alginate solution. The suspension should be uniform in consistency and free from any noticeable silica agglomerates to prevent blockages within the electrospraying tubing and/or nozzle.

4.2.4. Preparation of Si-SPs via Electrospraying

Si-SPs are synthesized using the electrospraying setup shown in Figure 9. The following example procedure details the synthesis of Si-SPs with a diameter of ~550 μm.

**NOTE:** Electrospraying and electrospinning are generally conducted using high-voltage power supplies that generate high voltage and current, thereby requiring regulated and safe practices to minimize risk of injury or death. As an added safety procedure, all electrospraying/electrospinning experiments within our research group have been conducted with a current of 0 A, with the setup encased within a lockable chamber (Figure 9b). Additional engineering controls, such as an automatic shutdown trip switch within the door frame, should also be considered.

A 30 mL plastic syringe is charged with the primary silica particles/alginate solution and positioned in a syringe pump programmed with a constant flow rate of 8 mL $h^{-1}$. A 17-gauge, blunt-tip needle is attached at the other end of a plastic tubing (5 mm in diameter) that feeds into the lockable chamber and is positioned vertically such that the distance from the tip of the needle to the surface of the $CaCl_2$ bath is 10 cm.

**NOTE:** A plastic-coated clamp and retort stand are used to secure the needle over the $CaCl_2$ bath to minimize the number of conductive components within the chamber. Prior to positioning the $CaCl_2$ bath beneath the needle, ensure the syringe is fully charged with no air pockets and gently inject the alginate solution through the tubing until it exits the needle. This is to ensure a constant flow rate through the tubing and encourage size homogeneity among the synthesized SPs. Furthermore, the needle should be as straight (vertical) as possible and not biased in any direction to encourage the formation of spherical SPs.

A voltage of 13 kV is applied to the top of the needle and the pump is switched on, generating a stream of droplets of the primary silica particles/alginate mixture that are collected in the gelling bath consisting of 1% w/v $CaCl_2$ dissolved in Milli-Q water. Cross-linking of the alginate is facilitated by $CaCl_2$, with visible micrometer-sized spheres forming in the gelling bath (Figure 10b).

4.2.5. Washing of Alginate/Si-SPs

The alginate/Si-SPs are retrieved from the gelling bath with a Pasteur pipette and transferred into a 50 mL Falcon® tube, into which 20 mL Milli-Q water is added. The lid is secured and the tube is gently rocked by hand to wash the supraparticles. The alginate/Si-SPs are allowed to sediment at the bottom of the tube, after which the washing liquid is removed and fresh Milli-Q water added. This process is repeated 4–5 times. The alginate/Si-SPs are subsequently transferred via Pasteur pipette into a porcelain dish, ensuring that the particles are lying on the flat portion of the dish (i.e., away from the walls) and are not in contact with one another. Excess water is removed by absorbing with a lint-free tissue (Kimwipe® or similar). Finally, alginate is removed via calcination at 923 K for 30 h (heating rate of 5 K $h^{-1}$) in air to yield Si-SPs (Figure 10c).

**NOTE:** Care must be taken when removing the alginate/Si-SPs from the gelling bath during washing and following calcination of the Si-SPs. This is to reduce the likelihood of particle cracking and defect formation (which are observed in Figure 10d) to thus obtain intact, spherical Si-SPs (Figure 10e). If porcelain dishes with curved walls, as the ones shown in Movie S3, are used, ensure that the alginate/Si-SPs are not touching or stacked upon one another when placed in the porcelain dishes prior to calcination to prevent the particles from fusing together. Furthermore, ensure that the particles are positioned as close as possible to the center of the dish. Particles that adhere to the curved walls of the dish may migrate/roll down the walls of the dish during calcination and come into contact with other SPs, leading to fusing or deformation.

4.3. Challenges and Considerations

The properties of the Si-SPs are summarized in Figure 10 and Table 4. Figure 10a shows a TEM image of the primary silica particles (850 ± 150 nm in diameter) prepared herein, displaying a characteristic mesoporous structure. These are smaller than those (~1 μm) reported by reported by Ma et al.[30] However, direct comparison is difficult as the standard deviations for the size, although apparent from the microscopy images, were not reported for the literature-synthesized particles. Nonetheless, the standard deviations of the primary silica particle diameters reported in this study overlap with the ~1 μm reported by Ma et al.[30] The alginate/Si-SPs can be seen in the collection dish containing the $CaCl_2$ gelling bath in Figure 10b. The calcined Si-SPs exhibited relatively uniform spherical structures (Figure 10c), with little variation in diameter and minimal signs of deformation or damage as confirmed by SEM (Figure 10d). An average Si-SP diameter of 517 ± 68 μm was determined, which is consistent with the average Si-SP diameter of 544 ± 41 μm reported by Ma et al.[30] An example of a damaged Si-SP is shown in Figure 10d, as evidenced from the flat indentation on the surface of the particle. The surface morphology of the calcined intact Si-SPs is shown in Figure 10f. The primary particle building blocks are evident along with the presence of voids. Furthermore, the decreasing trend in the zeta potential values of the Si-SPs with increasing pH (Figure 10g) is consistent with the zeta potential values and trend reported by Ma et al.[30] The data strongly support the adaptability of the electrospraying method to other electrospraying setups and its ability to produce increased volumes of Si-SPs.

Given that the scalability of the electrospraying method is determined by the capacity of the syringe and the flow rate during electrospraying, and that the equipment remains the same regardless of synthesis scale, the practicalities concerning large-scale synthesis are not significantly different from the smaller-scale synthesis. The parameters used in this study (flow rate: 8 mL $h^{-1}$; collector distance: 10 cm; applied voltage: 13 kV; primary silica particle concentration: 40 mg $mL^{-1}$) yielded 2000–2500 supraparticles in 1 h, a 3.5–4× increase over the 450–700 SPs/h prepared by Ma et. al.[30] The main differences between the two experimental protocols were the volume of primary silica particles/alginate solution electrosprayed per hour (2 mL for Ma et al.[30] and 8 mL in the present protocol) and the aforementioned optimized experimental parameters. A detailed study of the correlation between experimental parameters (i.e., concentration of alginate, concentration of primary silica particles, flow rate, applied voltage, and distance between the nozzle, and the surface of the gelling bath) and the properties of the SPs were presented by Ma et al.[30] Such factors can be readily controlled at all scales, highlighting the robustness of the technique. However, there are several additional considerations not

**Table 4. Comparison of large-scale experimental data and laboratory-scale reference data for Si-SPs prepared via gel-mediated electrospray**

| Property | Large-scale experimental data | Laboratory-scale reference data[a] |
|---|---|---|
| Yield | 2000–2500 SPs/h | 400–750 SPs/h[b] |
| Primary particle diameter (TEM) | 850 ± 150 nm | ~1 µm |
| Supraparticle diameter (SEM) | 517 ± 68 µm | 544 ± 41 µm |

[a]The reference data were obtained from Ma et al.[30]

[b]Yield data were not reported in Ma et al.[30] Thus, the experiments were replicated and the yield was determined visually.

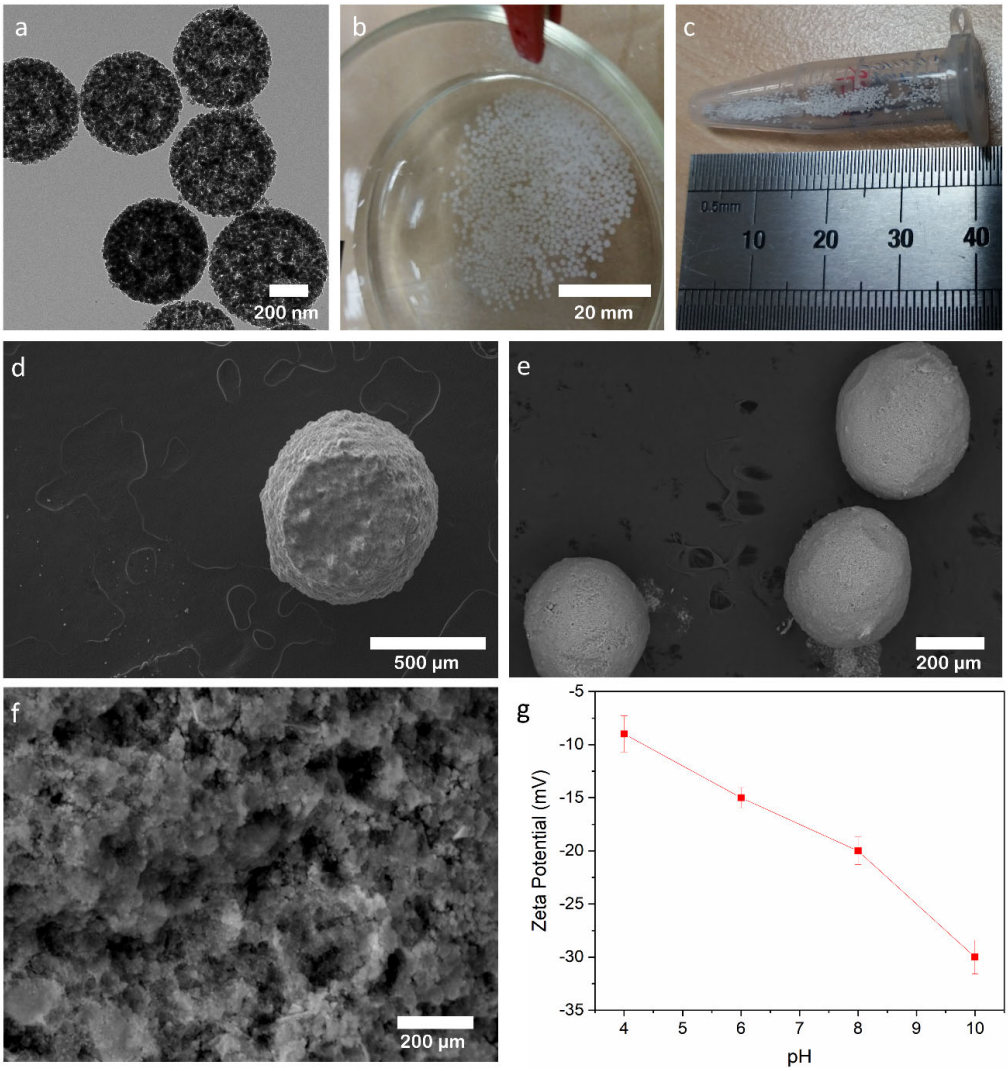


**Figure 10.** (a) TEM image of synthesized primary silica particles. (b) Cross-linked alginate/Si-SPs collected in the $CaCl_2$ gelling bath following electrospraying. (c) Calcined Si-SPs. SEM images of (d) a deformed, non-spherical calcined Si-SP, and (e) intact, spherical Si-SPs and (f) their surface. (g) Zeta potential values of the Si-SPs as a function of pH.

discussed by Ma et al.[30] that are as important to ensure reproducible fabrication of Si-SPs at increased yields as detailed below and summarized in Table 2.

*(i) Dispersion of Silica Primary Particles in Alginate Solution*

The methodology used to prepare the silica primary particles affords a particle yield of ~2 g, which is appropriate for dispersion in 50 mL of alginate solution. However, for a given primary silica particle/alginate mixture concentration, effective dispersion of the primary silica particles throughout the alginate solution may be limited at increased solution volumes. This is due to the viscous nature of the particles/alginate solution and limitations of the ultrasonication efficiency of baths when using larger vessels with increased solution volumes. For instance, in the present study, adequate distribution of the primary silica particles in completely filled 15 mL Falcon® tubes was achieved with ultrasonication for 1 h. In contrast, dispersion in completely

filled 50 mL tubes was challenging, requiring sonication times of more than 1 h. However, halving the volume (in the 50 mL tube) resulted in successful dispersion within 1 h. Therefore, using larger tubes that are not completely filled with particles/alginate solution or preparing several smaller (e.g., 15 mL) tubes in series can mitigate the chance of particle agglomeration at increased volumes.

*(ii) Electrospraying Device Configuration*

The assembly of the electrospraying device presents several considerations that can influence the shape and size homogeneity of the supraparticles. Therefore, these settings need to be appropriately controlled to ensure reproducible supraparticle fabrication. Firstly, the use of a sealed chamber to house the electrospraying assembly, aside from preventing electrocution, promotes a controlled environment (i.e., temperature and humidity) for SP formation and prevents human (e.g., accidental bumping of the needle or collection dish) or environmental (e.g., draft/flow from air conditioning) anomalies from interfering with the electrospraying process. Ensuring that the tubing and needle are completely charged with the primary silica particles/alginate solution and free of air pockets prior to switching on the pump is essential to prevent flow irregularities and needle sputtering, which can cause SP shape irregularities. In addition to the aforementioned distance between the nozzle and gelling bath surface, the orientation of the needle is important to prevent particles from exiting the nozzle biased toward any particular direction during extrusion. By maintaining the needle as straight (perpendicular to the surface of the benchtop) as possible, formation of a spherical SP free from deformations is encouraged. Finally, to promote a consistent voltage difference between the nozzle and gelling bath, it is recommended that the wires contact the nozzle and gelling bath at identical points every time the setup is used, and the number of conductive components within the vicinity of the nozzle is kept to a minimum. Thus, to minimize the chance of disruption or interference of the applied voltage from adjacent objects, we recommend the use of glass or nonconductive ceramic collection dishes, wooden or nonconductive plastic stands, and nonconductive plastic clamps.

*(iii) SP Harvesting, Washing, and Calcination*

Harvesting of the alginate/Si-SPs from the gelling bath and their subsequent washing is a key step in the fabrication process, as these gel-like SPs can be easily and unintentionally deformed with minimum force. A plastic Pasteur pipette with the tip cut at the point where it begins to narrow is highly recommended to gently and carefully remove the alginate/Si-SPs from the gelling bath and subsequently from the Falcon® tube following washing. Taking these steps during SP handling is essential to ensure that the SPs remain defect-free and intact. Slow and gentle rocking of the SPs during washing is also necessary to minimize the chance of deformation. This can be achieved manually or with a test-tube rocker or similar device operating at low speed.

The calcination process presents additional challenges that can lead to particle deformation or agglomeration. Aside from the care required in the aforementioned Pasteur pipette technique to place the SPs in the porcelain dish, ensuring that particles do not contact with one another when placed in the dish is important. This is to prevent fusing of SPs during calcination. Similarly, when porcelain dishes with curved walls (such as those shown in Figure S1) are used, the SPs should be placed on the flat portion of the dish away from the walls. SPs that adhere to the walls while still wet may roll/migrate during calcination, leading to potential defect formation or fusing with neighboring SPs. To eliminate the likelihood of SP migration while also increasing the number of particles that can be calcined within a single dish, dishes with non-curved wall edges are recommended. Finally, the calcined SPs require a gentle touch when being removed from the porcelain dish to prevent cracking or chipping following calcination. A 200 or 1000 μL pipette tip or similar utensil can be used to gently move the particles into a storage tube for subsequent use.

*(iv) Time Considerations*

Larger-scale fabrication of SPs involves increased time and human resource demands (specifically, removal of SPs from the gelling bath, washing and placing the SPs into porcelain dishes for calcination). Process monitoring is also required to ensure that any blockages within the tubing or nozzle are cleared promptly, that the applied voltage remains constant, and that the sample collection dish does not overfill. Although effective planning, time management, and (where possible) sharing and distribution of tasks can significantly reduce these constraints, the ability to stop the electrospraying process and start at a later point in time provides the greatest degree of flexibility and freedom in fabrication. Following device shutdown, syringes can be stored and ultrasonicated again prior to recommencing the electrospraying procedure. The process can undergo various start–stop iterations, without impacting the properties of the SPs. A key recommendation would be to flush the tubing and nozzle with water following each stoppage to reduce the risk of blockage formation and ensure that the tubing/nozzle are completely charged with solution and free from air bubbles before recommencing electrospraying.

## 5. CONCLUSIONS AND OUTLOOK

The processes involved in particle fabrication are often important in determining the property profiles and subsequently the quality of the particles and their applicability. This is particularly the case when upscaling of existing laboratory-scale protocols is attempted, with a direct scaling of volumes seldom yielding material properties similar to those of products prepared at smaller scales. The synthesis protocols of three particle systems used within our laboratory were described in detail to facilitate increased-scale, reproducible fabrication of these particles. Relative to the existing smaller-scale synthesis protocols, increases in yield per tube of 463× and 2× were achieved for MPNs prepared via discrete assembly onto PS particles and self-assembly on oil/water emulsions, respectively, using the larger-scale synthesis protocols developed herein. For the gel-mediated electrospraying larger-scale synthesis protocol developed, a 3.5–4× increase in Si-SP yield per hour was obtained. All particle and capsule systems were successfully prepared at increased scale without significant deviations in particle/capsule properties. A detailed, step-by-step protocol was documented for each particle system with accompanying video footage. Challenges and considerations associated with large-scale synthesis were discussed, with various strategies and solutions proposed and guidelines provided to promote particle property reproducibility. The protocols and supplementary videos were designed with the goal of explaining the synthesis procedure in such a manner that a

researcher without any prior particle engineering experience could successfully and reproducibly fabricate the particles with the desired properties. Increased yields were successfully obtained without significant deviation in material properties, highlighting the robust nature and potential for further scaling of these synthesis techniques.

Clear protocols are essential for method validation, adaptation of technologies and materials, and future development. By providing a protocol and video footage that detail each step and commentary on key steps, which may seem arbitrary to the novice researcher (e.g., centrifugation, pipetting), the likelihood of successful and reproducible synthesis is greatly increased. Likewise, benchmarking with existing, validated protocols is crucial to ensuring desired products and that desired material properties are obtained. Dividing a protocol into key steps can help determine crucial factors or conditions required to obtain successful material synthesis, while also aiding with troubleshooting and optimization. This may also make the overall process of protocol development more streamlined and time efficient. We believe that this strategy is applicable to a broad range of particle synthesis systems and can serve as a starting point to help determine crucial steps, synthesis parameters, and potential bottlenecks/challenges.

In addition, method accessibility and research transparency are important to facilitate material application, method validation, and development of future technologies. By providing a detailed and readily accessible methodology, our aim is to encourage the use and application of these particle systems, and provide avenues for further method development and optimization (including pilot-scale synthesis), and potentially a stepping stone for the development of new particle systems and synthesis technologies.

## ASSOCIATED CONTENT

**Supporting Information.** Particle system characterization, video protocols for Fe-TA MPN synthesis via discrete assembly, Fe-PEG-polyphenol MPN synthesis via self-assembly on oil/water emulsions, and Si-SP synthesis via gel-mediated electrospraying. This material is available free of charge via the Internet at http://pubs.acs.org.

## AUTHOR INFORMATION

### Corresponding Author

* Email: fcaruso@unimelb.edu.au

### Author Contributions

The manuscript was written through contributions of all authors. All authors have given approval to the final version of the manuscript.

## ACKNOWLEDGMENT

This research was conducted and funded by the Australian Research Council Centre of Excellence in Convergent Bio-Nano Science and Technology (project number CE140100036). F.C. acknowledges the award of a National Health and Medical Research Council Senior Principal Research Fellowship (GNT1135806). This work was performed in part at the Materials Characterisation and Fabrication Platform (MCFP) and Melbourne Advanced Microscopy Facility at The University of Melbourne, and the Victorian Node of the Australian National Fabrication Facility (ANFF). Transmission electron microscopy analyses were conducted using the facilities at the Biosciences Microscopy Unit, School of Bioscience, The University of Melbourne. We thank A./Prof. Hirotaka Ejima, and Drs Quinn A. Besford, Yutian Ma, Mattias Björnmalm, Joseph J. Richardson, and Christian Cortez-Jugo for helpful discussions, and Drs Matthew Faria and Aleksandr Kakinen for assistance with editing the video footage.

## REFERENCES

1. Ping, Y.; Guo, J.; Ejima, H.; Chen, X.; Richardson, J. J.; Sun, H.; Caruso, F. pH-Responsive Capsules Engineered from Metal–Phenolic Networks for Anticancer Drug Delivery. *Small* **2015**, *11*, 2032–2036.

2. Liang, H.; Li, J.; He, Y.; Xu, W.; Liu, S.; Li, Y.; Chen, Y.; Li, B. Engineering Multifunctional Films Based on Metal-Phenolic Networks for Rational pH-Responsive Delivery and Cell Imaging. *ACS Biomater. Sci. Eng.* **2016**, *2*, 317–325.

3. Hu, F.; Liu, B.; Chu, H.; Liu, C.; Li, Z.; Chen, D.; Li, L. Real-Time Monitoring of pH-Responsive Drug Release Using a Metal-Phenolic Network-Functionalized Upconversion Nanoconstruct. *Nanoscale* **2019**, *11*, 9201–9206.

4. Wang, C.; Sang, H.; Wang, Y.; Zhu, F.; Hu, X.; Wang, X.; Wang, X.; Li, Y.; Cheng, Y. Foe to Friend: Supramolecular Nanomedicines Consisting of Natural Polyphenols and Bortezomib. *Nano Lett.* **2018**, *18*, 7045–7051.

5. Dong, C.; Wang, Z.; Wu, J.; Wang, Y.; Wang, J.; Wang, S. A Green Strategy to Immobilize Silver Nanoparticles onto Reverse Osmosis Membrane for Enhanced Anti-Biofouling Property. *Desalination* **2017**, *401*, 32–41.

6. Ju, Y.; Cui, J.; Müllner, M.; Suma, T.; Hu, M.; Caruso, F. Engineering Low-Fouling and pH-Degradable Capsules through the Assembly of Metal-Phenolic Networks. *Biomacromolecules* **2015**, *16*, 807-814.

7. Besford, Q. A.; Ju, Y.; Wang, T.-Y.; Yun, G.; Cherepanov, P. V.; Hagemeyer, C. E.; Cavalieri, F.; Caruso, F. Self-Assembled Metal–Phenolic Networks on Emulsions as Low-Fouling and pH-Responsive Particles. *Small* **2018**, *14*, 1802342.

8. Zheng, H.-T.; Bui, H. L.; Chakroborty, S.; Wang, Y.; Huang, C.-J. Pegylated Metal-Phenolic Networks for Antimicrobial and Antifouling Properties. *Langmuir* **2019**, *35*, 8829–8839.

9. Wang, X.; Yan, J.; Pan, D.; Yang, R.; Wang, L.; Xu, Y.; Sheng, J.; Yue, Y.; Huang, Q.; Wang, Y.; Wang, R.; Yang, M. Polyphenol–Poloxamer Self-Assembled Supramolecular Nanoparticles for Tumor NIRF/PET Imaging. *Adv. Healthcare Mater.* **2018**, *7*, 1701505.

10. Chen, Y.; Wang, J.; Liu, J.; Lu, L. Metal-Phenolic Encapsulated Mesoporous Silica Nanoparticles for pH-Responsive Drug Delivery and Magnetic Resonance Imaging. *Z. Phys. Chem.* **2018**, *232*, 1733.

11. Zhu, W.; Liang, S.; Wang, J.; Yang, Z.; Zhang, L.; Yuan, T.; Xu, Z.; Xu, H.; Li, P. Europium-Phenolic Network Coated $BaGdF_5$ Nanocomposites for Tri-Modal Computed Tomography/Magnetic Resonance/Luminescence Imaging. *J. Mater. Sci.: Mater. Med.* **2017**, *28*, 74.

12. Guo, J.; Ping, Y.; Ejima, H.; Alt, K.; Meissner, M.; Richardson, J. J.; Yan, Y.; Peter, K.; von Elverfeldt, D.; Hagemeyer, C. E. Engineering Multifunctional Capsules through the Assembly of Metal–Phenolic Networks. *Angew. Chem. Int. Ed.* **2014**, *53*, 5546–5551.

13. Yang, C.; Wu, H.; Yang, X.; Shi, J.; Wang, X.; Zhang, S.; Jiang, Z. Coordination-Enabled One-Step Assembly of Ultrathin, Hybrid Microcapsules with Weak pH-Response. *ACS Appl. Mater. Interfaces* **2015**, *7*, 9178–9184.

14. Han, P.; Shi, J.; Nie, T.; Zhang, S.; Wang, X.; Yang, P.; Wu, H.; Jiang, Z. Conferring Natural-Derived Porous Microspheres with Surface Multifunctionality through Facile Coordination-Enabled Self-Assembly Process. *ACS Appl. Mater. Interfaces* **2016**, *8*, 8076–8085.

15. Yang, C.; Wu, H.; Shi, J.; Wang, X.; Xie, J.; Jiang, Z. Preparation of Dopamine/Titania Hybrid Nanoparticles through

Biomimetic Mineralization and Titanium(IV)–Catecholate Coordination for Enzyme Immobilization. *Ind. Eng. Chem. Res.* **2014**, *53*, 12665–12672.

16. Jia, X.; Wu, J.; Lu, K.; Li, Y.; Qiao, X.; Kaelin, J.; Lu, S.; Cheng, Y.; Wu, X.; Qin, W. Organic–Inorganic Hybrids of Fe–Co Polyphenolic Network Wrapped $Fe_3O_4$ Nanocatalysts for Significantly Enhanced Oxygen Evolution. *J. Mater. Chem. A* **2019**, *7*, 14302–14308.

17. Chen, W.; Hu, Y. Multiple Modifications of $BiVO_4$ through the Assembly of Metal-Phenolic Networks for Enhanced Photocatalytic Activity. *Catal. Commun.* **2019**, *123*, 124–128.

18. Li, X.; Gao, P.; Tan, J.; Xiong, K.; Maitz, M. F.; Pan, C.; Wu, H.; Chen, Y.; Yang, Z.; Huang, N. Assembly of Metal–Phenolic/Catecholamine Networks for Synergistically Anti-Inflammatory, Antimicrobial, and Anticoagulant Coatings. *ACS Appl. Mater. Interfaces* **2018**, *10*, 40844–40853.

19. Qin, Y.; Wang, J.; Qiu, C.; Hu, Y.; Xu, X.; Jin, Z. Self-Assembly of Metal–Phenolic Networks as Functional Coatings for Preparation of Antioxidant, Antimicrobial, and pH-Sensitive-Modified Starch Nanoparticles. *ACS Sustainable Chem. Eng.* **2019**, *7*, 17379–17389.

20. Kang, J.; Bai, G.; Ma, S.; Liu, X.; Ma, Z.; Guo, X.; Wang, X.; Dai, B.; Zhou, F.; Jia, X. On-Site Surface Coordination Complexation Via Mechanochemistry for Versatile Metal–Phenolic Networks Films. *Adv. Mater. Interfaces* **2019**, *6*, 1801789.

21. Luo, W.; Xiao, G.; Tian, F.; Richardson, J. J.; Wang, Y.; Zhou, J.; Guo, J.; Liao, X.; Shi, B. Engineering Robust Metal–Phenolic Network Membranes for Uranium Extraction from Seawater. *Energy & Environ. Sci.* **2019**, *12*, 607–614.

22. Kim, H. J.; Kim, D.-G.; Yoon, H.; Choi, Y.-S.; Yoon, J.; Lee, J.-C. Polyphenol/$Fe^{III}$ Complex Coated Membranes Having Multifunctional Properties Prepared by a One-Step Fast Assembly. *Adv. Mater. Interfaces* **2015**, *2*, 1500298.

23. Paliwal, R.; Babu, R. J.; Palakurthi, S. Nanomedicine Scale-Up Technologies: Feasibilities and Challenges. *AAPS PharmSciTech* **2014**, *15*, 1527–34.

24. Baer, D. R. The Chameleon Effect: Characterization Challenges Due to the Variability of Nanoparticles and Their Surfaces. *Front. Chem.* **2018**, *6*, 145–145.

25. Charitidis, C. A.; Georgiou, P.; Koklioti, M. A.; Trompeta, A.-F.; Markakis, V. Manufacturing Nanomaterials: From Research to Industry. *Manuf. Rev.* **2014**, *1*, 11.

26. Tighe, C. J.; Cabrera, R. Q.; Gruar, R. I.; Darr, J. A. Scale Up Production of Nanoparticles: Continuous Supercritical Water Synthesis of Ce–Zn Oxides. *Ind. Eng. Chem. Res.* **2013**, *52*, 5522–5528.

27. Park, J.; An, K.; Hwang, Y.; Park, J.-G.; Noh, H.-J.; Kim, J.-Y.; Park, J.-H.; Hwang, N.-M.; Hyeon, T. Ultra-Large-Scale Syntheses of Monodisperse Nanocrystals. *Nat. Mater.* **2004**, *3*, 891–895.

28. Pileni, M. P. Au Supracrystal Growth Processes: Unexpected Morphologies. *Bull. Chem. Soc. Jpn.* **2019**, *92*, 312–329.

29. Björnmalm, M.; Cui, J.; Bertleff-Zieschang, N.; Song, D.; Faria, M.; Rahim, M. A.; Caruso, F. Nanoengineering Particles through Template Assembly. *Chem. Mater.* **2017**, *29*, 289–306.

30. Ma, Y.; Björnmalm, M.; Wise, A. K.; Cortez-Jugo, C.; Revalor, E.; Ju, Y.; Feeney, O. M.; Richardson, R. T.; Hanssen, E.; Shepherd, R. K.; Porter, C. J.; Caruso, F. Gel-Mediated Electrospray Assembly of Silica Supraparticles for Sustained Drug Delivery. *ACS Appl. Mater. Interfaces* **2018**, *10*, 31019–31031.

31. Ejima, H.; Richardson, J. J.; Liang, K.; Best, J. P.; van Koeverden, M. P.; Such, G. K.; Cui, J.; Caruso, F. One-Step Assembly of Coordination Complexes for Versatile Film and Particle Engineering. *Science* **2013**, *341*, 154–157.

32. Ejima, H.; Richardson, J. J.; Caruso, F. Metal-Phenolic Networks as a Versatile Platform to Engineer Nanomaterials and Biointerfaces. *Nano Today* **2017**, *12*, 136–148.

33. Dai, Q.; Yu, Q.; Tian, Y.; Xie, X.; Song, A.; Caruso, F.; Hao, J.; Cui, J. Advancing Metal–Phenolic Networks for Visual Information Storage. *ACS Appl. Mater. Interfaces* **2019**, *11*, 29305–29311.

34. Zhong, Q.-Z.; Li, S.; Chen, J.; Xie, K.; Pan, S.; Richardson, J. J.; Caruso, F. Oxidation-Mediated Kinetic Strategies for Engineering Metal–Phenolic Networks. *Angew. Chem. Int. Ed.* **2019**, *58*, 12563–12568.

35. Pan, S.; Guo, R.; Bertleff-Zieschang, N.; Li, S.; Besford, Q. A.; Zhong, Q.-Z.; Yun, G.; Zhang, Y.; Cavalieri, F.; Ju, Y.; Goudeli, E.; Richardson, J. J.; Caruso, F. Modular Assembly of Host–Guest Metal–Phenolic Networks Using Macrocyclic Building Blocks. *Angew. Chem. Int. Ed.* **2020**, *59*, 275–280.

36. Ju, Y.; Cortez-Jugo, C.; Chen, J.; Wang, T.-Y.; Mitchell, A. J.; Tsantikos, E.; Bertleff-Zieschang, N.; Lin, Y.-W.; Song, J.; Cheng, Y.; Mettu, S.; Rahim, M. A.; Pan, S.; Yun, G.; Hibbs, M. L.; Yeo, L. Y.; Hagemeyer, C. E.; Caruso, F. Engineering of Nebulized Metal–Phenolic Capsules for Controlled Pulmonary Deposition. *Adv. Sci.* **2020**, *7*, 1902650.

37. Ahn, S.; Halake, K.; Lee, J. Antioxidant and Ion-Induced Gelation Functions of Pectins Enabled by Polyphenol Conjugation. *Int. J. Bio. Macromol.* **2017**, *101*, 776–782.

38. Rahim, M. A.; Björnmalm, M.; Bertleff-Zieschang, N.; Ju, Y.; Mettu, S.; Leeming, M. G.; Caruso, F. Multiligand Metal–Phenolic Assembly from Green Tea Infusions. *ACS Appl. Mater. Interfaces* **2018**, *10*, 7632–7639.

39. Ju, Y.; Dai, Q.; Cui, J.; Dai, Y.; Suma, T.; Richardson, J. J.; Caruso, F. Improving Targeting of Metal–Phenolic Capsules by the Presence of Protein Coronas. *ACS Appl. Mater. Interfaces* **2016**, *8*, 22914–22922.

40. Ju, Y.; Cui, J.; Sun, H.; Müllner, M.; Dai, Y.; Guo, J.; Bertleff-Zieschang, N.; Suma, T.; Richardson, J. J.; Caruso, F. Engineered Metal-Phenolic Capsules Show Tunable Targeted Delivery to Cancer Cells. *Biomacromolecules* **2016**, *17*, 2268–2276.

41. Yun, G.; Besford, Q. A.; Johnston, S. T.; Richardson, J. J.; Pan, S.; Biviano, M.; Caruso, F. Self-Assembly of Nano- to Macroscopic Metal–Phenolic Materials. *Chem. Mater.* **2018**, *30*, 5750–5758.

42. Yun, G.; Richardson, J. J.; Biviano, M.; Caruso, F. Tuning the Mechanical Behavior of Metal–Phenolic Networks through Building Block Composition. *ACS Appl. Mater. Interfaces* **2019**, *11*, 6404–6410.

43. Guo, J.; Richardson, J. J.; Besford, Q. A.; Christofferson, A. J.; Dai, Y.; Ong, C. W.; Tardy, B. L.; Liang, K.; Choi, G. H.; Cui, J. Influence of Ionic Strength on the Deposition of Metal–Phenolic Networks. *Langmuir* **2017**, *33*, 10616–10622.

44. Rahim, M. A.; Ejima, H.; Cho, K. L.; Kempe, K.; Müllner, M.; Best, J. P.; Caruso, F. Coordination-Driven Multistep Assembly of Metal–Polyphenol Films and Capsules. *Chem. Mater.* **2014**, *26*, 1645–1653.

45. Richardson, J. J.; Cui, J.; Björnmalm, M.; Braunger, J. A.; Ejima, H.; Caruso, F. Innovation in Layer-by-Layer Assembly. *Chem. Rev.* **2016**, *116*, 14828–14867.

46. Richardson, J. J.; Liang, K.; Kempe, K.; Ejima, H.; Cui, J.; Caruso, F. Immersive Polymer Assembly on Immobilized Particles for Automated Capsule Preparation. *Adv. Mater.* **2013**, *25*, 6874–6878.

47. Björnmalm, M.; Yan, Y.; Caruso, F. Engineering and Evaluating Drug Delivery Particles in Microfluidic Devices. *J. Controlled Release* **2014**, *190*, 139–149.

48. Ma, J.; Lee, S. M.-Y.; Yi, C.; Li, C.-W. Controllable Synthesis of Functional Nanoparticles by Microfluidic Platforms for Biomedical Applications – A Review. *Lab Chip* **2017**, *17*, 209–226.

49. Weiss, A. C.; Kempe, K.; Förster, S.; Caruso, F. Microfluidic Examination of the "Hard" Biomolecular Corona Formed on Engineered Particles in Different Biological Milieu. *Biomacromolecules* **2018**, *19*, 2580–2594.

50. Liu, Z.; Le, Z.; Lu, L.; Zhu, Y.; Yang, C.; Zhao, P.; Wang, Z.; Shen, J.; Liu, L.; Chen, Y. Scalable Fabrication of Metal–Phenolic Nanoparticles by Coordination-Driven Flash Nanocomplexation for Cancer Theranostics. *Nanoscale* **2019**, *11*, 9410–9421.

51. del Mercato, L. L.; Ferraro, M. M.; Baldassarre, F.; Mancarella, S.; Greco, V.; Rinaldi, R.; Leporatti, S. Biological Applications of LbL Multilayer Capsules: From Drug Delivery to Sensing. *Adv. Colloid and Interface Sci.* **2014**, *207*, 139–154.

52. Yang, Y.; Wang, J.; Shigematsu, H.; Xu, W.; Shih, W. M.; Rothman, J. E.; Lin, C. Self-Assembly of Size-Controlled Liposomes on DNA Nanotemplates. *Nat. Chem.* **2016**, *8*, 476–483.

53. Zang, Z.; Wen, M.; Chen, W.; Zeng, Y.; Zu, Z.; Zeng, X.; Tang, X. Strong Yellow Emission of ZnO Hollow Nanospheres Fabricated Using Polystyrene Spheres as Templates. *Mater. Des.* **2015**, *84*, 418–421.

54. Zhang, H.; Nayak, S.; Wang, W.; Mallapragada, S.; Vaknin, D. Interfacial Self-Assembly of Polyelectrolyte-Capped Gold Nanoparticles. *Langmuir* **2017**, *33*, 12227–12234.

55. Nador, F.; Guisasola, E.; Baeza, A.; Villaecija, M. A. M.; Vallet-Regí, M.; Ruiz-Molina, D. Synthesis of Polydopamine-Like Nanocapsules Via Removal of a Sacrificial Mesoporous Silica Template with Water. *Chem. – Eur. J.* **2017**, *23*, 2733–2733.

56. Parakhonskiy, B. V.; Yashchenok, A. M.; Möhwald, H.; Volodkin, D.; Skirtach, A. G. Release from Polyelectrolyte Multilayer Capsules in Solution and on Polymeric Surfaces. *Adv. Mater. Interfaces* **2017**, *4*, 1600273.

57. Ma, M.; Xu, H.; Chen, H.; Jia, X.; Zhang, K.; Wang, Q.; Zheng, S.; Wu, R.; Yao, M.; Cai, X.; Li, F.; Shi, J. A Drug–Perfluorocarbon Nanoemulsion with an Ultrathin Silica Coating for the Synergistic Effect of Chemotherapy and Ablation by High-Intensity Focused Ultrasound. *Adv. Mater.* **2014**, *26*, 7378–7385.

58. Fotticchia, T.; Vecchione, R.; Scognamiglio, P. L.; Guarnieri, D.; Calcagno, V.; Di Natale, C.; Attanasio, C.; De Gregorio, M.; Di Cicco, C.; Quagliariello, V.; Maurea, N.; Barbieri, A.; Arra, C.; Raiola, L.; Iaffaioli, R. V.; Netti, P. A. Enhanced Drug Delivery into Cell Cytosol Via Glycoprotein H-Derived Peptide Conjugated Nanoemulsions. *ACS Nano* **2017**, *11*, 9802–9813.

59. Hörmann, K.; Zimmer, A. Drug Delivery and Drug Targeting with Parenteral Lipid Nanoemulsions — A Review. *J. Controlled Release* **2016**, *223*, 85–98.

60. Dai, Y.; Guo, J.; Wang, T.-Y.; Ju, Y.; Mitchell, A. J.; Bonnard, T.; Cui, J.; Richardson, J. J.; Hagemeyer, C. E.; Alt, K.; Caruso, F. Self-Assembled Nanoparticles from Phenolic Derivatives for Cancer Therapy. *Adv. Healthcare Mater.* **2017**, *6*, 1700467.

61. Li, Y.; Xiang, D. Stability of Oil-in-Water Emulsions Performed by Ultrasound Power or High-Pressure Homogenization. *PLoS One* **2019**, *14*, e0213189.

62. Xia, Y.; Yin, Y.; Lu, Y.; McLellan, J. Template-Assisted Self-Assembly of Spherical Colloids into Complex and Controllable Structures. *Adv. Funct. Mater.* **2003**, *13*, 907–918.

63. Chen, K.; Liang, F.; Lu, X.; Xue, D. Toward Materials-by-Design: Achieving Functional Materials with Physical and Chemical Effects. *Nanotechnology* **2019**, *31*, 024002.

64. Dai, Q.; Bertleff-Zieschang, N.; Braunger, J. A.; Björnmalm, M.; Cortez-Jugo, C.; Caruso, F. Particle Targeting in Complex Biological Media. *Adv. Healthcare Mater.* **2018**, *7*, 1700575.

65. Cui, J.; Richardson, J. J.; Björnmalm, M.; Faria, M.; Caruso, F. Nanoengineered Templated Polymer Particles: Navigating the Biological Realm. *Acc. Chem. Res.* **2016**, *49*, 1139–1148.

66. Sperling, M.; Gradzielski, M. Droplets, Evaporation and a Superhydrophobic Surface: Simple Tools for Guiding Colloidal Particles into Complex Materials. *Gels* **2017**, *3*, 15.

67. Phillips, K. R.; England, G. T.; Sunny, S.; Shirman, E.; Shirman, T.; Vogel, N.; Aizenberg, J. A Colloidoscope of Colloid-Based Porous Materials and Their Uses. *Chem. Soc. Rev.* **2016**, *45*, 281–322.

68. Rastogi, V.; Melle, S.; Calderón, O. G.; García, A. A.; Marquez, M.; Velev, O. D. Synthesis of Light-Diffracting Assemblies from Microspheres and Nanoparticles in Droplets on a Superhydrophobic Surface. *Adv. Mater.* **2008**, *20*, 4263–4268.

69. Yeo, S. J.; Tu, F.; Kim, S.-h.; Yi, G.-R.; Yoo, P. J.; Lee, D. Angle- and Strain-Independent Coloured Free-Standing Films Incorporating Non-Spherical Colloidal Photonic Crystals. *Soft Matter* **2015**, *11*, 1582–1588.

70. Rastogi, V.; Velev, O. D. Development and Evaluation of Realistic Microbioassays in Freely Suspended Droplets on a Chip *Biomicrofluidics* **2007**, *1*, 014107.

71. Xu, S.; Weng, Z.; Tan, J.; Guo, J.; Wang, C. Hierarchically Structured Porous Organic Polymer Microspheres with Built-in $Fe_3O_4$ Supraparticles: Construction of Dual-Level Pores for Pt-Catalyzed Enantioselective Hydrogenation. *Polym. Chem.* **2015**, *6*, 2892–2899.

72. Gao, W.; Wang, J. The Environmental Impact of Micro/Nanomachines: A Review. *ACS Nano* **2014**, *8*, 3170–3180.

73. Rastogi, V.; Velikov, K. P.; Velev, O. D. Microfluidic Characterization of Sustained Solute Release from Porous Supraparticles. *Phys. Chem. Chem. Phys.* **2010**, *12*, 11975–11983.

74. Ma, W.-F.; Wu, K.-Y.; Tang, J.; Li, D.; Wei, C.; Guo, J.; Wang, S.-L.; Wang, C.-C. Magnetic Drug Carrier with a Smart pH-Responsive Polymer Network Shell for Controlled Delivery of Doxorubicin. *J. Mater. Chem.* **2012**, *22*, 15206–15214.

75. Wang, Y.; Wise, A. K.; Tan, J.; Maina, J. W.; Shepherd, R. K.; Caruso, F. Mesoporous Silica Supraparticles for Sustained Inner-Ear Drug Delivery. *Small* **2014**, *10*, 4244–4248.

76. Maina, J. W.; Cui, J.; Björnmalm, M.; Wise, A. K.; Shepherd, R. K.; Caruso, F. Mold-Templated Inorganic–Organic Hybrid Supraparticles for Codelivery of Drugs. *Biomacromolecules* **2014**, *15*, 4146–4151.

Table of content graphic